Nanoparticle Synthesis

DOI: 10.1002/anie.201402986

Thermodynamics versus Kinetics in Nanosynthesis

*Yawen Wang, Jiating He, Cuicui Liu, Wen Han Chong, and Hongyu Chen**

Keywords:
hybrid structures · kinetics · micelles · nanoparticle synthesis · thermodynamics

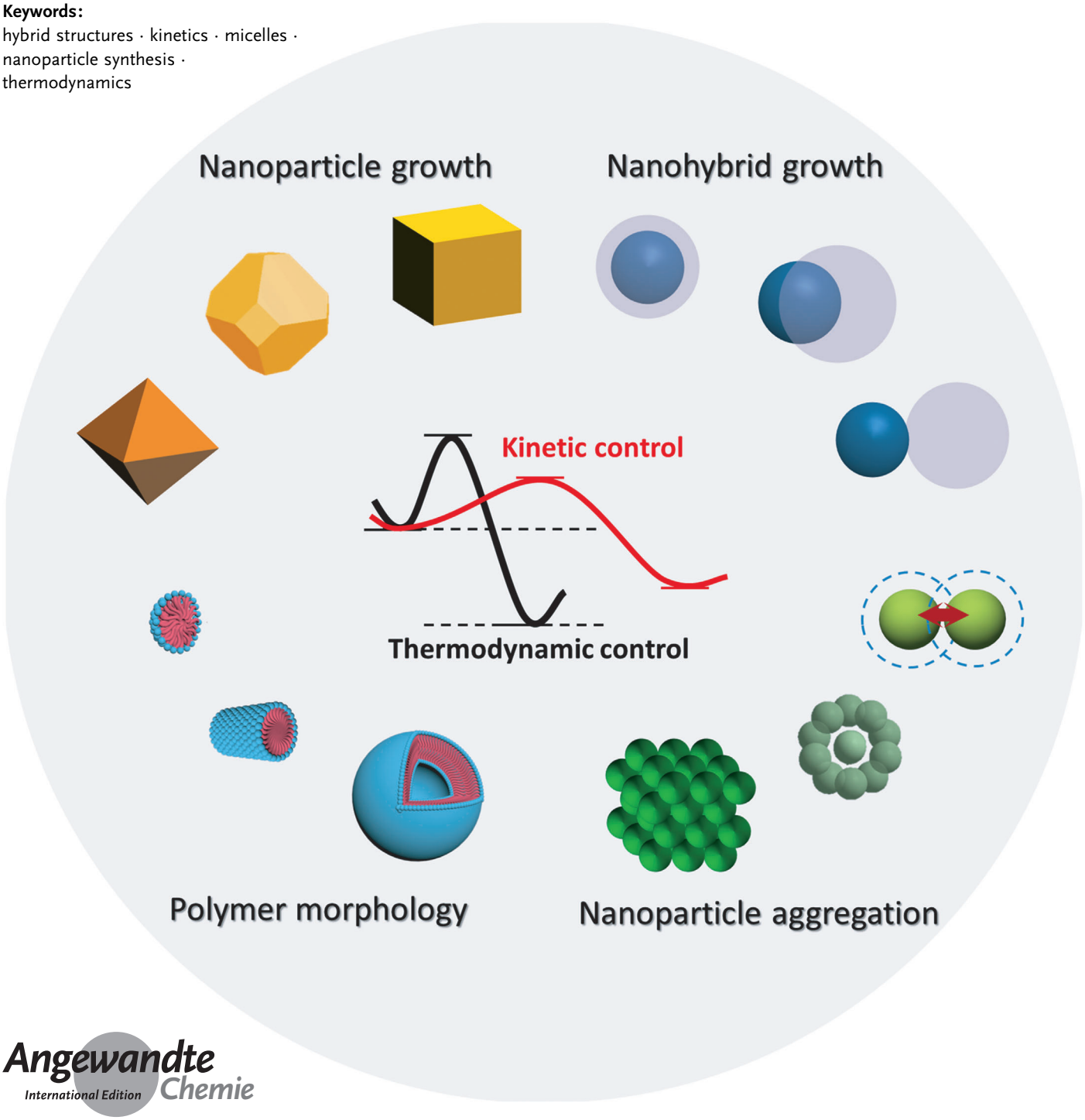

One may discover a stone tool by chance but it takes more than luck to make a car or cell phone. With the advance of nanoscience, the synthesis of increasingly sophisticated nanostructures demands a rational design and a systems approach. In this Review, we advocate the distinction between thermodynamically and kinetically controlled scenarios, that is, whether a product forms because it is the most stable state or because the pathway leading to it has the lowest energy barrier. Great endeavours have been made to describe the multiple concurrent processes in typical nanosynthesis phenomena, so that the mechanistic proposals in the literature are brought into a common framework for easy contrast and comparison.

From the Contents

1. Introduction

Thermodynamics deals with the driving force of a system moving from the initial state to the product state, whereas kinetics is concerned with the energy barriers of the specific pathways in this process.

Although thermodynamic and kinetic analyses are common in the traditional fields of chemical science,[1] they are rare in nanoscience to date. The key issue is to evaluate the relative stability of the starting materials, intermediates, and products. As will be discussed in the following, it is actually possible to compare the various forms of nanostructures by using simple standards, such as the surface to volume (S/V) ratio and the strength of interactions. Such analyses are beginning to provide insights for designing synthetic pathways for sophisticated nanostructures.

1.1. Thermodynamics versus Kinetics in Chemical Science

For a typical chemical reaction, one often needs to distinguish whether it is thermodynamically or kinetically controlled,[1b,2] in other words, whether the product forms because it is the most stable state or because the pathway leading to it has the lowest energy barrier (the energy cost at the transition state). This problem is hereafter referred to as the T-K problem. In the first case, the choice of the products is compared independent of the reaction pathways, whereas the latter is concerned with the choice of pathways resulting from different reaction rates.

Understanding such a distinction is crucial for achieving a fundamental understanding and for controlling the synthesis. It would be preposterous, for example, if only equations with thermodynamic factors were enlisted to fit the data, when actually the reaction was kinetically controlled. In a simple illustration, Figure 1 shows the potential energy landscape of two competitive reactions, where C is the thermodynamically favored product and D is the kinetically favored one. The rate constant is exponentially dependent on the activation energy E_a [Eq. (2)].[3] Thus, the reaction corresponding to the red pathway is significantly faster and leads to D as the main product. On the other hand, if an equilibrium is established, the molecules will experience the different product states multiple times and eventually accumulate at the most stable state. The equilibrium constant is exponentially dependent on the driving force $\Delta G°$ [Eq. (1)], thus making C the main product.[3]

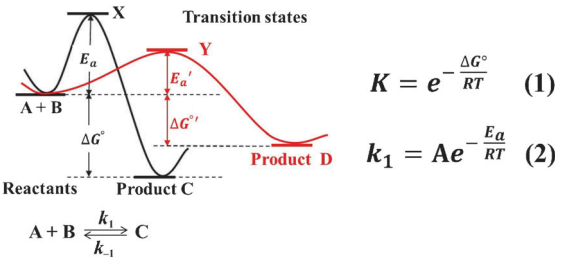

Figure 1. Simple energy landscape illustrating the choice between the thermodynamically and kinetically controlled products.

When studying a kinetically controlled reaction, one needs to identify the rate-limiting step and understand the transition state therein. Creating new pathways (e.g. by using catalysts) and manipulating the interactions at the intermediate states would be more important than devising methods to stabilize the product. To increase the yield, one should lower the temperature just enough for the reaction to proceed, and isolate the product as soon as it is finished, so that the competitive and the reverse reactions can be suppressed. In contrast, when synthesizing the thermodynamically controlled product, one should increase the reaction temperature and allow sufficient time so that the reaction can approach equilibrium. To increase the yield, conditions can be selected to destabilize the starting materials and/or stabilize the product.

[*] Y. Wang, J. He, C. Liu, W. H. Chong, Prof. H. Chen
Division of Chemistry and Biological Chemistry
Nanyang Technological University
21 Nanyang Link, Singapore 637371 (Singapore)
E-mail: hongyuchen@ntu.edu.sg
Homepage: http://www.ntu.edu.sg/home/hongyuchen/

The conventional methods of analysis, for example, calorimetry,[1a,3,4] cannot be easily applied to the typical problems in nanosynthesis. For example, the coalescence of two Au nanospheres with $d = 15.9$ nm into a product sphere of $d = 20$ nm results in the number of surface atoms decreasing from about 22000 to 17000 (Figure 2). Assuming that each internal atom has 12 bonded neighbors (in a fcc lattice) and each surface atom has 9 (on (111) facets), there is a gain of 7000 metallic bonds on coalescence. Given there is a total of 253000 atoms in the system, the thermodynamic driving force is about 0.026 Au–Au bonds per atom, which is much less than the driving force of a typical chemical reaction. The driving force would be even smaller if the coalescence was incomplete, and if bonding interactions with the surface ligands were considered.

Although the young field of nanoscience has yet to catch up with the mature fields of physical chemistry, simple geometric analysis and logical deduction can provide powerful predictions, which can then be subjected to experimental verification.

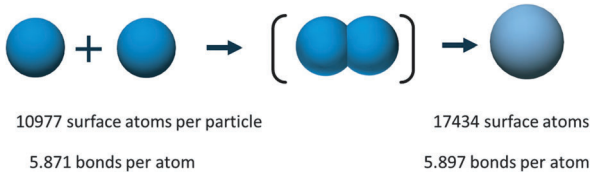

Figure 2. Difficulty in measuring the calorimetric changes on coalescence of two small Au nanospheres ($d = 15.9$ nm) into one larger sphere ($d = 20$ nm). The enthalpy change per atom would be hard to detect.

1.2. Two Explanations for a Simple Phenomenon

What would be one's reaction to the simple question: "How come the cell phone dropped to the ground"? To answer "because on the ground it has the lowest potential energy" would be a funny, but true, answer. Although the gravitational field of the Earth provides the driving force, it is not an answer one would normally expect. More often than not, we are interested in the kinetic barrier and the course of action, that is, what prevents the cell phone from dropping in the first place and what leads to its free fall.

Thus, there are at least two explanations to any phenomenon, namely, the nature of the thermodynamic driving force and the nature of the kinetic barrier. Since any spontaneous process must be thermodynamically favorable, it may seem that the thermodynamic explanation is unnecessary. However, the goal of mechanistic study is to provide predictive power (Figure 3), which would be partially lost if either of the answers is missing. Having a tendency to drop to the ground does not mean the cell phone will necessarily do so, and

Yawen Wang was born in Zhejiang, China. She obtained her BSc from the Division of Chemistry & Biological Chemistry at Nanyang Technological University in Singapore in 2010. She then joined the group of Prof. Hongyu Chen as a PhD candidate in the same year. Her research interests include controlled synthesis of noble metal nanostructures and nanocomposites.

Jiating He was born in Guangdong, China. He obtained his BSc in 2006 and MSc in 2009 from the Department of Chemistry, Jilin University in China. In 2014, he obtained his PhD in the Division of Chemistry & Biological Chemistry at Nanyang Technological University under the supervision of Prof. Hongyu Chen. His research interests include the synthesis and application of noble metal nanomaterials.

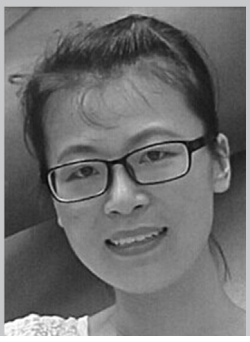

Cuicui Liu was born in Jiangsu, China. She obtained her BSc in 2006 and MSc in 2009 from College of Chemistry in Soochow University. She joined the Division of Chemistry & Biological Chemistry at Nanyang Technological University in Singapore and obtained her PhD under the supervision of Prof. Hongyu Chen in 2013. Her research interests include the controlled self-assembly of block copolymers and their combination with noble metal nanoparticles.

Wen Han Chong was born in Perak, Malaysia. After obtaining his BSc from the Division of Chemistry and Biological Chemistry at Nanyang Technological University in Singapore, he joined the group of Prof. Hongyu Chen as a PhD candidate in 2010. His main research interest is in the controlled self-assembly of core–shell magnetic nanostructures.

Hongyu Chen obtained his BSc from the University of Science and Technology of China (USTC) in 1998. He studied Mn complexes and water oxidation chemistry at Yale University. After obtaining his PhD in 2004, he worked as a postdoctoral fellow at Cornell University on the topic of protein–nanoparticle hybrids. In 2006, he joined the Division of Chemistry and Biological Chemistry at Nanyang Technological University in Singapore, where he is currently an Associate Professor. His main research interest is the development of new synthetic methods for nanostructures.

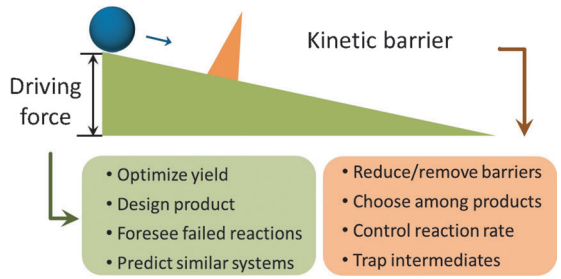

Figure 3. The goal of understanding thermodynamics and kinetics is to provide rational predictions. Lacking one branch means there is missing predictive power.

removing the kinetic barrier does not necessarily mean it would drop. Without a gravitational field it would float.

1.3. The T-K Problem

In a typical experiment, an interesting result is observed (e.g. nanocrystals with a certain shape) and a key experimental parameter noted (e.g. ligand concentration). One may explain that the ligands stabilize a particular set of facets, thus leading to the shape of the nanocrystals. While this statement may be correct, it is certainly not a complete explanation. In the mechanistic proposal, it should be conveyed whether the stabilized facets lead to the most stable final product or to the most favorable pathway towards the product (for example, the preferential growth at unstable facets, see Section 3.3.3). Mixing these incompatible arguments would be very confusing. Similar to chemical reactions, the thermodynamically and kinetically controlled scenarios are drastically different, with distinctive consequences and controlling methods.

We argue that making such a distinction is essential for a mechanistic study. In experiments, recognizing the nature of the thermodynamic driving force and of the kinetic barrier is critical for circumventing problems and exploring innovative approaches. When formulating a theory, producing equations without resolving the T-K problem can easily confuse a reader, if not the authors themselves.

1.4. Process Analysis

The T-K problem is only the first step in analyzing the overall process. An initial hypothesis would at least remove the ambiguity, so that one can interpret the various factors affecting the observables under a specific scenario. The deductions from the analysis, when feasible, can then be tested by experiments.

While the thermodynamic analysis only needs to consider the starting and ending states, the kinetic analysis is all about the detailed process, that is, how the various factors interact with each other, and how exactly these interactions lead to what is observed. Given the complexity, it would be impractical to characterize all of the states along the different pathways. There are often multiple concurrent processes in a typical nanosynthesis phenomenon, unlike a typical chemical reaction. To treat the overall process as a "black box" for data interpretation is too coarse and often incorrect.

The typical approach in chemistry is to establish the mechanistic hypothesis on the basis of a few key observables, making sure it is also consistent with the control experiments and the trapped intermediates. The critical step is to design specific experiments to test the hypothesis against the alternative explanations. In nanoscience, great attention has traditionally been paid to the physical characterization of nanocrystals. Notwithstanding the importance of the shape and internal structure, a static state is often not a sufficient basis for interpreting the overall process. We should emulate the chemistry approach to check the hypothetical predictions against the experimental observables. In this Review, we endeavor to describe the distinct scenarios and to categorize the possible explanations, so as to facilitate contrast and comparison in mechanistic studies. As detailed in the following, recognizing the different processes and logically combining their effects is essential for mechanistic analysis.

1.5. Scope of this Review

We use the term "nanosynthesis" to designate the overall field of colloidal synthesis, which involves the growth, etching, assembly, and shape transformation of nanostructures. In contrast, the term "chemical synthesis" refers to the creation of compounds by molecular reactions, and the term "nanofabrication" traditionally refers to the engineering of nanoscale features on bulk substrate surface, often involving cleanroom techniques.[5]

We apply thermodynamic and kinetic analysis to typical problems in nanosynthesis. The aim is to deconvolute the problems and summarize the logical mechanistic proposals in a common framework for easy contrast and comparison. As such, the focus of this Review is not the synthetic details but the underlying principles. To avoid overlap, existing reviews will be cited but not discussed in detail.

2. Standards for Evaluation

As shown in Figure 1, the key process in thermodynamic and kinetic analysis is to compare the relative stability of the initial, intermediate, and product states. In a chemical reaction, the stability of the molecules is usually evaluated on the basis of bond energy and computational simulations, for example.[6] However, the same standards cannot be easily applied in nanosynthesis.

Typical nanostructures contain a huge number of atoms and so a comparison of the bonding interactions has to be carried out in a different manner. For metallic clusters with less than 100 atoms, calorimetry and computer simulation are still manageable. Indeed, their detailed thermodynamic and kinetic analyses have been carried out and reviewed.[1a,7] However, for nanoparticles with thousands of atoms (a 3.2 nm Au NP has about 1000 atoms), conventional methods of simulation would be too costly in terms of computation time. Thus, new methods are required.[8]

Moreover, unlike molecules with identical composition, a collection of NPs, regardless of how uniform, always has a certain distribution in terms of size, shape, surface-ligand density, and even chemical composition. Lastly, in typical phenomena, such as growth, aggregation, and morphological evolution, there are uncertainties at the molecular level. For example, during aggregation, the contact area between the NPs and the ligand density therein are of critical importance to the stability of the resulting cluster, but such properties are highly variable in the mixture and very difficult to characterize.

Even with these limitations, thermodynamic and kinetic analysis is still possible by focusing on the dominant factors and major trends. In this Review, we will discuss a few possible means to evaluate the relative stability of nanostructures. With advance of the field, more standards that are suitable for the particular nature of the problems in nanosynthesis will hopefully be developed.

2.1. Type and Strength of Interactions

For a NP suspended in a solution, there are cohesive interactions within the NP as well as surface interactions with the environment. Depending on the material, the cohesive interactions include metallic, covalent, or ionic bonding, van der Waals interactions, hydrogen bonding, etc. The surface atoms may interact directly with the environment or through ligands. Thus, the surface interactions include NP–solvent, NP–ligand, ligand–ligand, and ligand–solvent interactions. In experimental studies (as opposed to computational simulations), it is often difficult to separate these interactions. In the following, we consider the surface energy as a whole, including the contributions from the ligands and interfacial defects. The NP–NP interactions (e.g. charge and dipole interactions) are also important for a collection of NPs.

Hydrophobic interactions often play important roles in nanoscience.[9] Taking the aggregation of two carbon nanotubes (CNTs) in water as an example, the process is favorable because it reduces the exposed surface area. The unaggregated CNTs are not stable because their inability to form hydrogen bonds leads to disruption of the highly dynamic hydrogen bonds between the water molecules. This restricts their mobility and results in a structured "cage" around the nonpolar surface (mostly of entropic nature because of the reduced freedom of the water molecules).[10] Although there are only van der Waals interactions between the CNTs in the product state, part of the stability of the aggregate originates from a reduction in the unfavorable CNT–water interactions of the initial state. Given the "invisible" contribution (there is no real hydrophobic force between the aggregated CNTs), the term "hydrophobic interaction" is typically used to designate the driving force of the overall system. This interaction is well-established in biological systems (e.g. in protein folding),[11] but not yet broadly recognized in the field of nanoscience.

As will be discussed in the main sections, one can often invoke the relative strength of interactions to compare the stability of different states. Given the variety and large number of interactions in nanostructures, it is important to compare both the quality and quantity of interactions. For example, the formation of defects in nanocrystals or the lattice mismatch between the neighboring domains reduces the number of bonding interactions therein (Section 4.1.1). The introduction of ionic polymer in hydrophobic domains leads to less-favorable polar–nonpolar interactions (Section 6.1). In both examples, the reduction in the interactions arising from the lower quality and/or quantity gives rise to unstable states. On the other hand, a better packing of the polymer chains in a domain leads to a larger number of cohesive interactions per unit amount of material (e.g. van der Waals interactions in polystyrene), but with an entropic penalty. The same logic can be applied when comparing the amorphous and crystalline states of the same material. In general, ordered packing is energetically favorable due to the dominant enthalpic contribution.

2.2. Surface Energy at the Nanoscale

In nanosynthesis, the surface energy is often the key contributing factor, because the amount of materials and their chemical composition do not typically change during aggregation, coalescence, or morphological evolution. In this context, when considering the possible states of NPs of different sizes and shapes, the main difference is the number of surface atoms/molecules, which have less favorable interactions than do the internal ones. To illustrate this point, we use a water droplet as a simple model (Figure 4).

A molecule on the surface of a water droplet has weak interactions with the surrounding air, but strongly hydrogen bonds with the neighboring molecules inside the droplet. Thus, on average it experiences a net force perpendicular to the water–air interface, namely, the surface tension. Balancing the surface tension around the droplet leads to a spherical shape. From a chemist's point of view, the surface molecules experience weaker interactions than the interior ones do (and an additional entropic term if they have less mobility). To maximize the favorable interactions within the droplet, it should minimize the number of surface molecules, that is, minimize its S/V ratio by forming a sphere (Figure 4). On the basis of this analysis, stronger cohesive interactions within a material should lead to a larger driving force during the minimization of its S/V ratio.

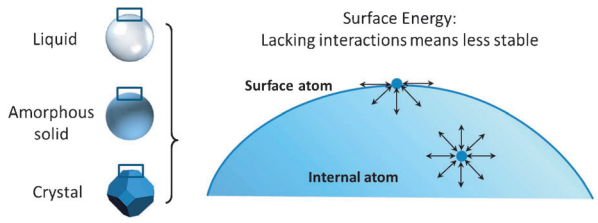

Figure 4. The essence of surface energy: Minimizing the energy of the system requires minimizing the number of the surface atoms with unfavorable interactions. This principle applies to all nanostructures, although the facets are also important in crystals.

Similarly, the spherical shape of nanometer-sized liquid droplets can also be explained on the basis of their surface energy. The higher percentage of surface molecules on a smaller domain will mean that the surface energy would play an even more significant role.[12] Mechanical analysis of surface tension is difficult for a solid NP, but it is conceivable that maximizing the cohesive interactions within the NP (metallic bonds, ionic bonds, etc.) would drive the system towards the minimized S/V ratio.

Considering the lower number of interactions on a surface, the surface energy is defined as the unit energy required to create a new surface.[13] As such, it is important to note that this energy is defined relative to the bulk energy, thus making it positive in value (unfavorable). In experiments, the surface often interacts with a medium (gas or solvent) or another solid; thus the surface energy is reduced (in quality and quantity) when there are strong surface interactions. In the following, we use the term "interfacial energy" instead of "surface energy" when emphasizing the interactions between the surface and its environment or the neighboring domain. Typically, the interactions between the surface and the media (solvent molecules) are weaker than the cohesive interactions within the NP,[3] otherwise the system would seek to maximize the solvent–NP interface, which means that the NPs would be dissolved.

The interface between two juxtaposed domains of condensed phase is an important component of the total interfacial energy. It basically depends on the strength of the interactions at the interface, more specifically on the quality of the bonding interactions between the domains, the matching of the opposing lattices (which affects the number of bonding interactions and/or bond distances), the interfacial defects, as well as entropic contributions. Such chemical analysis can provide an alternative perspective to the wetting properties that are extensively discussed in physics. For a liquid droplet on a solid surface, the liquid domain would adopt a configuration with minimized total interfacial energy or, equivalently, one with maximized total bonding interactions. If there are only weak bonding interactions at the solid–liquid interfaces, maximizing the cohesive interactions within the droplet would become a better option. This prevents the droplet from spreading out, thereby leading to a poor wetting property. Detailed analysis will be discussed in Section 4.

In short, while interfacial energies are difficult to measure for nanostructures, we can deduce the major trends by comparing them on the basis of bonding interactions. For many structures, the S/V ratio is a convenient standard, which, admittedly, is not as rigorous as the interfacial energy. However, in contrast to the latter, it can be easily calculated from the experimentally observed structures.

3. Growth of Single-Domain Nanoparticles

3.1. Effects of Ligands

Ligands play a pivotal role in the synthesis of NPs. The process of a ligand binding to a NP surface has a thermodynamic driving force and encounters kinetic barriers,[14] which should not be confused with the thermodynamic and kinetic factors of nanocrystal growth, which will be discussed in this section.

The affinity of a ligand for a NP surface depends not only on the chemical bonding at the anchoring point, but also on the ligand–ligand packing interactions.[15] Basically, ligands crowded in a patch have to break the interactions with their neighbors, which makes it more difficult for them to dissociate. Thus, the size and orderliness of the ligand patch are of importance, because better packing leads to more effective ligand–ligand interactions. A consequence of this argument is that the size and shape of NPs become relevant factors, because the size of the ligand patch depends on the size of the underlying facet.

In a colloidal solution, ligands dynamically adsorb to and detach from the NP surface.[16] In their presence, the growth of the underlying facet is attenuated because the growth materials cannot be directly deposited on top of the ligands (a few exceptions involving the incorporation of defects in nanocrystals should be noted).[17] The deposition of material has to "wait" until ligand dissociation exposes the crystal surface. Thus, the ligand affinity determines the "on"/"off" ratio of the ligand,[18] which in turn governs the rate of facet growth (the kinetics).

Interacting both with the solvent and with the crystal surface, the ligand layer also modulates the thermodynamic stability of the facets, thereby influencing the end states of the nanocrystal growth.

3.2. Thermodynamic Analysis

The common explanation for the shape of a NP is that "it is stable". However, without comparison with its alternative shapes, this statement carries little information, as anything that forms must be energetically more favorable than the starting materials ($\Delta G < 0$). To evaluate the stability of NPs, one needs to compare the different end states (e.g. cube/cuboid), the choice of facets, and the sharpness or roundedness of the edges and corners.

For simplicity, we first analyze the surface energy of one nanocrystal with an invariant volume (no growth or aggregation). In comparison to liquid droplets and amorphous NPs, the minimization of the surface energy in nanocrystals is more complex because they have different types of facets. The facets have different densities of surface atoms, charges, and ligands, which leads to different stabilities.

If all of the facets of a nanocrystal are equally favored, then a spherical shape would be preferred because it has the lowest S/V ratio (Figure 5). At the other extreme, a polyhedron with sharp edges and corners will be preferred if only *one* type of facet is favored, for example, octahedra with (111) facets, cubes with (100) facets, etc. Most nanocrystals lie in between these two extremes, with a range of surface energies for the different types of facets. When the difference in the stability of the facets is reduced, more than one type of facet will appear and the resulting polyhedron should gradually appear rounder, with truncated edges and corners.

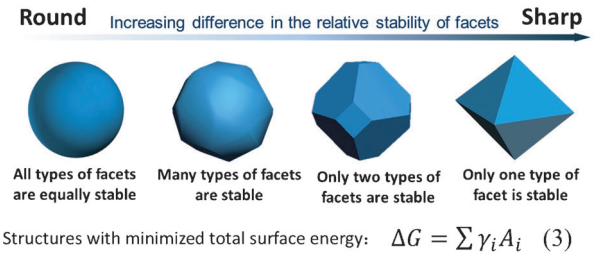

Figure 5. The lowest energy structure of a nanocrystal can vary, depending on the relative stability of its facets.

The system seeks to minimize the total surface energy, that is, the sum of the facet area weighted by their respective surface energy [Eq. (3)].

$$\Delta G = \Sigma \gamma_i A_i \quad (3)$$

Here, γ is the surface energy of a given facet and A is its area (Figure 5). Thus, we arrive at the classic Wulff construction (the Gibbs–Wulff Theorem).[19] In experiments, the observation of nanocrystals adopting rounder shapes is sometimes associated with the removal of the ligand or a reduction of its concentration. This reduces the difference in the stability between the facets, thus leading to less sharp edges and corners.

The Wulff construction considers the equilibrium shape of nanocrystals and is, therefore, a thermodynamic concept and should not be applied to kinetically controlled structures. It should be noted that the relative stability of the facets of nanocrystals is often interpreted on the sole basis of the observed shapes, whereas in bulk crystals the surface energies are measureable. Thus, directly reapplying facet stability to explain the shape of nanocrystals can sometimes lead to circular arguments.

Without considering ligand modification, the relative stability of the facets can be evaluated on the basis of the bonding interactions within the facets, which depends on the surface packing efficiency. Basically, a facet is more stable when, on average, an atom thereon has more and/or stronger bonds. In fcc metal nanocrystals, for example, the (111) facets are normally the most stable ones, because the atoms thereon have the largest number of neighbors. On this basis, it is generally agreed that $\gamma_{(111)} < \gamma_{(100)} < \gamma_{(110)} <$ other higher index facets.[20] For ionic crystals, charge balance is of great importance. For example, NaCl crystals prefer the (100) facets over (111) facets, because the former are charge neutral whereas the latter are dominated by one type of charge. In contrast to the idealized "clean" facets, the surface ligand is an important factor, if not the dominant one, for most of the colloidal nanocrystals. Indeed, a wide variety of ligands are known in the literature to stabilize the specific facets of nanocrystals.[21]

It is not always easy to determine if the formation of a nanocrystal is thermodynamically or kinetically controlled. A rule of thumb is that those with high aspect ratio are likely not the most stable form, in particular, when there is inequivalent growth of the equivalent facets. In single-crystalline fcc nanocrystals, for example, there are always multiple equivalent facets (eight (111) facets, six (100) facets, etc.). Without invoking additional factors (Section 3.4), they should remain equivalent. It would be implausible to invoke enormously different surface energies to explain the large difference in the respective facet areas (Wulff construction) for some nanowires (NWs) and nanorods with high aspect ratio. In other words, should a NW flow like a liquid, it would withdraw into a near spherical polyhedron to reduce its S/V ratio. A faceted grain with an equal area of the equivalent facets should be more favorable than a wire with a high aspect ratio (Figure 5).

On the other hand, determining the thermodynamically favored shape of semiliquid (e.g. polymer NPs formed above their glass transition temperature) or amorphous NPs is easy. Without the influence of facets, the S/V ratio is a good standard of evaluation.

3.2.1. *Means To Achieve Thermodynamic Control*

In chemical reactions, the thermodynamically controlled product is obtained when the system is in equilibrium. In contrast, there are several different scenarios whereby a NP can reach its minimal energy shape (Figure 6): 1) the NP is

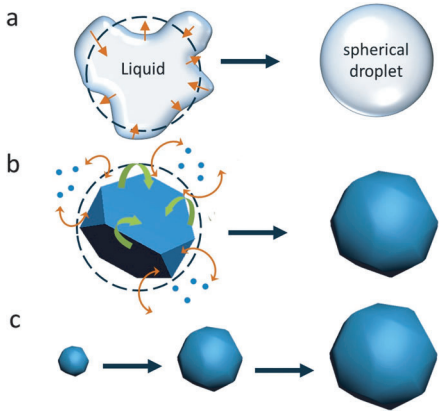

Figure 6. Different scenarios to achieve minimal energy structures: a) by the flowing of liquid; b) by the dynamic dissolving and re-depositing of the growth material (brown arrows) or the rapid migration of the surface atoms (green arrows); and c) when the minimal energy form is achieved in every step.

a liquid or has sufficient structural fluidity (e.g. malleability in metallic structures), so that it can flow into the minimal energy shape; 2) the material of the NPs is continuously dissolving and re-depositing, thereby reaching an equilibrium; 3) the surface atoms are rapidly migrating, equilibrating the external facets;[22] 4) during the growth of the NP, its shape has the minimal energy in every step, so that the final shape is also thermodynamically controlled. It should be noted that there are differences in these equilibria. For example, the internal defects are easily adjusted in scenario 1, but not in scenarios 2, 3, and 4 (see Section 3.4). Moreover, the dissolution/re-deposition equilibrium will lead to the exchange of materials among the NPs (Ostwald ripening), thus giving a broad size distribution.

The shape transformation of nanostructures typically involves the transfer of materials across great distances (tens of nm or longer), such as during the fusion of NWs into NPs or the conversion of tetrahedra into spheres. As such, the structural transformation of the unit cell (diffusionless or martenstic transformation)[23] would be insufficient to account for the changes at the longer distances.

The detailed steps in reaching the lowest energy shape can be subjected to kinetic analysis. The lack of prominent barriers in some cases could mean that the driving forces are subtle and accumulative. For example, in the shape evolution of an irregular droplet into a sphere (Figure 6a), the interfacial tension pushes the droplet towards gradually more favorable forms. If one analyzes at the molecular level over a very short time interval, the dynamic process would seem random. However, the thermodynamic control is like "invisible hands" that provide the direction of progress, where the exact pathway is hard to predict and often meaningless. After the droplet has oscillated a few times, it would eventually settle at the spherical shape. Similarly, despite the dynamic and chaotic steps in forming the spherical NPs atom by atom, the underlying thermodynamic control may exert its effects in a subtle and consistent manner.

3.2.2. *Defining the Right System*

Proper definition is of great importance when discussing "the minimum energy state of NPs". The discussion in Section 3.2 only considers a single NP and its ligands, because they contribute to the facet stability.

If we consider all the NPs in the solution, the collection is clearly not at the minimum energy state, regardless of the shape of the NPs. The system would seek the minimum total surface energy by reducing the number of particles. Ostwald ripening is a possible means to exchange materials among the NPs and reduce the energy of the system.[24] In this context, the thermodynamically stable final state would be one giant particle with a minimized surface.

The discussion on thermodynamics can be confusing if the boundaries are ill-defined. For example, if the NPs can react with the residual reactants, air, or water in the environment, their chemical instability can further complicate the discussion of shapes. In principle, the definition is critically dependent on what is included in the system and the applicable time frame.

In many cases, we are interested in the shape of the colloidal NPs, not their chemical changes. In practice, the product NPs can be isolated before they have enough time to ripen or degrade. In this Review, when discussing the minimum energy state of NPs, we only consider the NPs individually, comparing them to their other potential shapes.

3.3. *Kinetic Analysis*

In contrast to the thermodynamics, the kinetics of NP growth is influenced by a variety of factors during the different steps of the fundamental processes, for example, the random encounter of the growth materials, the formation of stable nuclei, and the isotropic diffusion of growth materials towards the nuclei. In the following, the effects are discussed separately.

Unlike an elementary chemical reaction, the above processes are complex with numerous elementary steps, for example the sequential addition of atoms during crystal growth. The concept of an activation barrier can be directly applied to the elementary addition of an atom, but there is a deviation when describing the "activation" barrier of the overall process. Our view is that the kinetic arguments can be qualitatively applied to analyzing an overall process, just like analyzing the rolling of a ball over a bump with a rough surface, provided that the overall barrier is much greater than those of the elementary steps. When the system is able to cross the overall barrier, it is possible that near equilibrium conditions are attained in the elementary steps.

During the growth of a nanocrystal, the atoms/molecules are deposited onto a nucleus, but it is also possible that they will re-dissolve in the solution or migrate on the surface. These processes are akin in concept to reverse chemical reactions. It is important to note that the reversibility is critical to the formation of facets. In a homogeneous solution, the diffusion of growth materials towards the nucleation center is isotropic in nature (on average or upon accumulation). For the facet stability to exert its influence, the growth material must sample at multiple locations, thus making re-dissolving a necessary condition. In other words, if the deposition is a one-way process, uniform over-coating will only lead to isotropic structures (spheres). Experimentally, at the beginning of the growth, the initial fast reaction rate typically leads to rapid deposition and negligible re-dissolution. Indeed, the intermediates trapped before the formation of faceted NPs (such as cubes and octahedra) are often smaller spheres.[25] In this context, the initial stage of nanosphere formation is kinetically controlled. At the later stage, a slower reaction rate and the dissolving/deposition dynamic would help establish the stable facets.

3.3.1. *Nucleation and Growth*

The typical growth of NPs shares a similar process, regardless of the composition of the material. A chemical reaction gives free atoms or molecules, which are then used in the growth. The basic process of how these free atoms or molecules join with each other has been described in the classic theory of nucleation and growth (Figure 7a).[18,21e,26]

Basically, there is a main kinetic barrier to forming nuclei in a homogeneous solution (the homogeneous nucleation).[27] It arises because the nuclei, being extremely small and not thoroughly solvated, are less stable than both the well-solvated atoms/ions and the subsequently formed larger NPs. The Gibbs free energy for forming a spherical nucleus can be expressed as the sum of the volume energy and the surface energy [Eq. (4)].[21e,27,28]

$$\Delta G = \frac{4}{3}\pi r^3 G_v + 4\pi r^2 \sigma \quad (4)$$

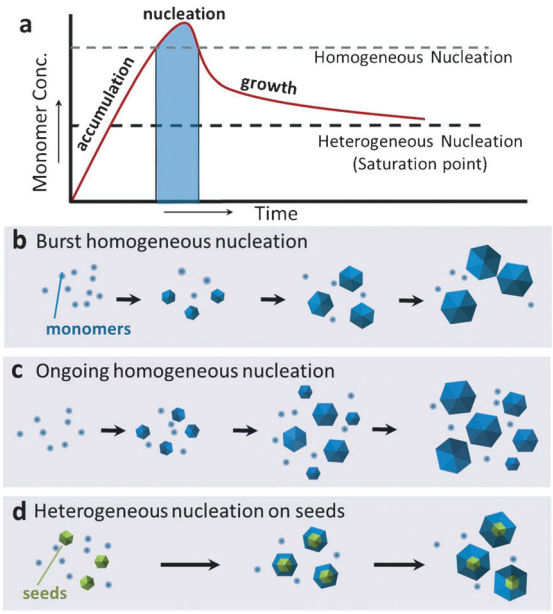

Figure 7. a) Plot of monomer concentration against time, illustrating the initial accumulation of the monomers, the nucleation stage, and the subsequent growth of the nuclei (modified from Ref. [21e, 26a] with permission. Copyright 2009 Wiley-VCH, 1950 American Chemical Society); b–d) kinetic analysis of crystal growth: b) all nuclei are generated at roughly the same time and grow at the same rate; c) with an over-supply of monomers, continual homogeneous nucleation leads to polydispersed NPs; d) heterogeneous nucleation occurs only on the pre-existing seeds.

Here, G_v is the energy per unit volume (negative), σ is the surface energy per unit area of the nucleus (positive), and r is the radius. Addition to the nucleus is energetically unfavorable until it reaches a critical radius. This inflection point can be described by Equation (5).

$$r^* = -\frac{2\sigma}{G_v} \tag{5}$$

Thus, for the overall growth (note the many elementary steps therein), the nucleation barrier is the amount of energy required to form a nucleus with the critical radius r^* [Eq. (6)].

$$\Delta G^* = \frac{16\pi\sigma^3}{3(G_v)^2} \tag{6}$$

This barrier forces the growth material to build up in the solution, thereby making the solution oversaturated (the accumulation stage, Figure 7a). Initially, the clusters formed by the random collision of the monomer species are too small to be stable. As a result, they dissolve in the solution and regenerate the monomers. As the oversaturation increases, a certain point is reached where the collision becomes so intense that many clusters are able to grow beyond the critical size, thereby giving stable nuclei (the nucleation stage) and consuming the growth materials. This stage only lasts for a short period until the oversaturation drops below the critical level, thereby stopping the formation of new nuclei. The deposition of the monomers on the stable nuclei (the heterogeneous nucleation) is energetically favorable, and the growth will last as long as the solution is oversaturated (the growth stage).

In experiments, the kinetic pathways of NP growth and control of the NP size distribution are mainly dependent on how the nucleation barrier is crossed. In an extreme case, the chemical reactions are instantaneously finished. The resulting oversaturation of the growth materials leads to rapid homogeneous nucleation. If there is no kinetic barrier for the nucleation, the aggregation of the monomer species would be similar to the step-growth polymerization of organic monomers,[29] thereby leading to polydispersed atomic clusters (see also Section 5.2). However, the kinetic barrier causes the initial clusters to re-dissolve, except those above the critical size, making the latter emerge from the nucleation uniform in size. A good example is the formation of noble metal NPs by the rapid reduction of metal salts using $NaBH_4$.[30] The nucleation consumes a significant portion of the monomer species, thus preventing continual homogeneous nucleation. Given the large number of nuclei and the diminished amount of growth materials, it would be difficult to grow large NPs. To this end, the use of more starting materials is usually not a good strategy, because their higher concentration would lead to faster initial reactions and thus a higher oversaturation. Therefore, the extra materials would contribute to an increased number of nuclei instead of additional growth on the individual NPs.

If the chemical reactions are still ongoing after the initial nucleation event, it is possible that they may build up enough growth materials for continuous homogeneous nucleation. Thus, the new nuclei that emerge later would have less time to grow, thereby leading to polydispersed NPs (Figure 7c). To achieve uniformly sized NPs, the rate of producing the growth materials should be kept slower than that of its consumption (heterogeneous nucleation on the existing nuclei). This prevents the build-up of material and suppresses the homogeneous nucleation, thus allowing all the nuclei to emerge at roughly the same time and to grow at the same rate (Figure 7b).

Temperature is a convenient variable for controlling the growth kinetics. Its main effect is on the reaction rates, although it also affects the saturation level of the growth material, reaction equilibrium, etc. The "hot-injection" method used for the synthesis of quantum dots is a good example.[31] The injection of a reactant at room temperature causes a major drop in the temperature (e.g. from 300° to 180° within seconds).[31b] With the initial burst nucleation and the rapid drop in reaction rates, the oversaturation is quickly brought below the critical level. The subsequent growth is dominated by the heterogeneous nucleation on the initial nuclei. The burst nucleation and the separation of the nucleation and growth processes, together with the "size-distribution focusing" effects, lead to NPs with extremely narrow size distributions.[18, 26b, 32]

3.3.2. *Seeding*

Given a same amount of starting material, the size of the resulting NPs is inversely proportional to the number of

nuclei in the system. However, it is usually very difficult to control the number of nuclei formed during the homogeneous nucleation. To solve this problem, prefabricated NPs can be used as seeds, so that the number of NPs in the solution can be predetermined. If all of the seeds grow at the same rate and there are no newly formed nuclei, the product NPs will have a uniform size distribution (Figure 7d).

The amount of seeds is also important. If the seed concentration is extremely low, there will be regions in the solution where the produced growth material cannot reach any seeds by diffusion.[33] It is also possible that severe aggregation of the NPs may greatly reduce the number of nucleation centers (in the form of clusters of NPs), which will lead to a similar situation. The consequence is the local build-up of the growth material, which causes homogeneous nucleation. The resulting nuclei will then participate in the subsequent growth, competing with the seeds, and resulting in NPs of different sizes. Whether such a build-up can occur depends on the seed concentration, the rate of mass transport (diffusion, convection, etc.), and the production/consumption dynamic of the growth material. Thus, stirring and the viscosity of the solution are also factors.

With this background knowledge, one can appreciate why nanoparticle syntheses are often less reproducible than chemical reactions. The homogeneous nucleation is highly sensitive to the experimental conditions, such as temperature, stirring (which affects the solution homogeneity), impurities (which lead to premature nucleation or aggregation of nuclei), etc. Such sensitivity could be responsible for the variation between different batches of syntheses.

3.3.3. Kinetic Control of Nanocrystal Shapes

The relative stability of the facets can be modulated by selecting facet-specific ligands or surfactants. It has been widely postulated that the preferential formation of stable facets is a result of rapid growth at the unstable facets.[21e,34] Basically, the atoms newly added to an unstable facet can establish better bonding interactions than those added to a stable facet can. The former process encounters a lower barrier and is thus faster [Eq. (2)]. Flanked by the stable facets, the filling of the unstable facets reduces and eventually eliminates their area, thus leading to nanocrystals with only stable facets. As proposed in the literature, polyvinylpyrrolidone (PVP) passivates Ag(100) facets and leads to Ag nanocubes;[25a,35] citrate ions passivate Ag(111) facets to yield Ag octahedra;[36] high-index facets such as the Au(221) facets can be generated in trisoctahedral nanocrystals by using hexadecyltrimethylammonium chloride (CTAC) as the ligand (Figure 8).[37]

In the thermodynamic arguments (Section 3.2), the emergence of facets depends on their relative stability. In contrast, the kinetic arguments here emphasize the relative rate of growth.[38] These two trends may or may not coincide. Considering the complex role of ligands, there is likely no simple interdependency. A possible test is by Ostwald ripening: If a system is merely kinetically controlled, incubating spherical NPs with the ligands would not give the desired facets.

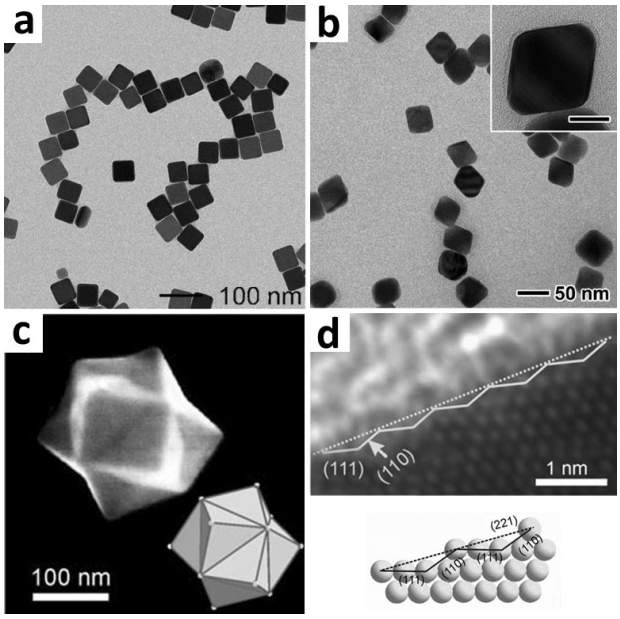

Figure 8. TEM images of a) 50 nm Ag nanocubes synthesized using PVP as the ligand; b) Ag octahedra obtained with sodium citrate as the ligand. The scale bar in the inset is 20 nm. c) SEM and d) HRTEM image of trisoctahedral nanocrystals and the model of a (221) facet. Reprinted from Refs. [25a, 36a, 37], respectively, with permission. Copyright 2010 Wiley-VCH, 2010 American Chemical Society, and 2008 Wiley-VCH.

3.3.4. Inducing Anisotropy in Nanocrystals

In the literature, many nanocrystals are highly anisotropic, with a rod, wire, or plate shape.[21e,34,39] As discussed in Section 3.2, such structures are likely thermodynamically unfavorable. The key to understanding the kinetic process is to identify the anisotropy factor that is responsible for the inequivalent growth of the equivalent facets.

While most lattices are intrinsically symmetric with multiple equivalent facets, the presence of defects can break their symmetry. The preferred growth at the defect sites (or unfavorable growth) thus induces anisotropy during the crystal growth (Figure 9). Specifically, if there is a stacking fault between the crystal planes ((111),[40] (100),[41] etc.), the growth along the fault plane at the edges would be more favorable than the deposition perpendicular to the plane, thus leading to platelike nanocrystals (Figure 9a,b). On the other hand, if a nucleus has a fivefold twinning defect, it can grow into a NW because longitudinal growth is preferred (Figure 9c,d).[42] Basically, the inability of the twinned domains to fill the space[43] leads to bond stretching and defects (i.e. the induced strain), which restrict the lateral growth of the NWs. Furthermore, the presence of a screw dislocation on a facet would greatly favor deposition of the material thereon, thus making its growth many times faster than the other seemingly equivalent facets. Thus, the unidirectional growth leads to highly anisotropic NWs or nanotubes (Figure 9e,f).[44]

The facet-specific binding of surface ligands may also induce the anisotropic growth of nanocrystals.[21c] It has been proposed that the effects are exerted by the selective

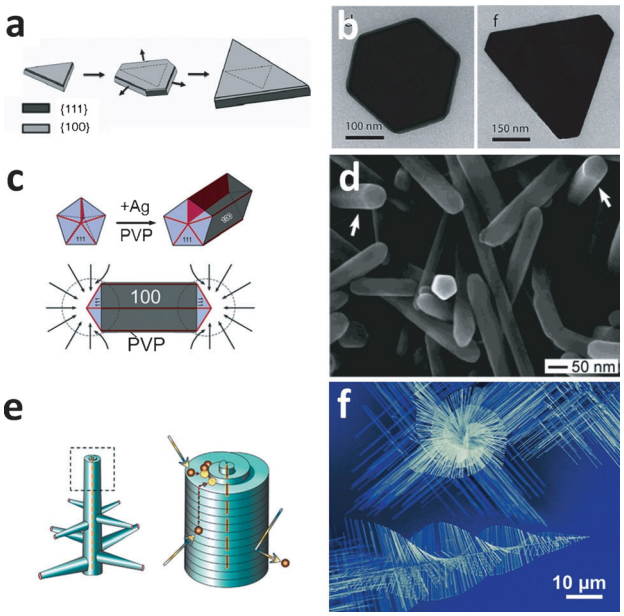

Figure 9. Defect-induced anisotropic growth. a,b) Schemetic representations and TEM images of Ag nanoplates, where the growth is promoted by the stacking fault between the (100) planes. c,d) The growth of Ag NWs as a result of the fivefold twinning defect and the favored (100) facets. e,f) The growth of ZnO "Christmas trees" driven by the screw-dislocation defect. Reprinted from Refs. [41c, 42, 44a], respectively, with permission. Copyright 2012 Wiley-VCH, 2005 American Chemical Society, and 2008 AAAS.

passivation of facets; for example, the binding of hexadecyltrimethylammonium bromide (CTAB) on the Au(100) surface leads to the formation of nanorods.[45] Similarly, the preferential adsorption of CO on Pd(111) facets was proposed to confine the Pd deposition between the two stabilized planes, thereby giving rise to ultrathin nanosheets.[46] On the other hand, amphiphilic ligands are proposed to form cylindrical micelles[47] that can template the formation of rod- or wirelike nanocrystals (see also Section 4.3).[39c,48] The cylindrical micelles break the symmetry among the equivalent facets, which leads to anisotropic growth. Such reported ligands include CTAB,[49] oleylamine,[50] and oleic acid.[51]

In the above two categories, defects and ligands are the anisotropy factors only after they come into existence. That is, the existing defects and ligand organization are already anisotropic before they promote the anisotropic crystal growth. To obtain a collection of uniform NPs, such factors must be consistently present in all the individual NPs. Thus, for many systems there is a gap in explaining the inequivalent growth of the equivalent facets, that is, how exactly the specific type of defects or specific ligand passivation are *consistently* generated in/on the initial symmetrical nuclei. A possible explanation is that those nanocrystals without the anisotropic factor are outcompeted and may either redissolve or remain in the sample as impurity nanocrystals.

In vapor-liquid-solid (VLS) or solution-liquid-solid (SLS) growth,[39a,52] the growth material is dissolved in the molten seed and the nucleation occurs specifically at the seed–nanocrystal interface. The molten seed defines the cross-sectional width of the emerging nanocrystal, thus making it the anisotropy factor. It thus promotes the unidirectional growth of the nanocrystals into NWs as opposed to plates or spheres. Recently, our group reported a system with a similar growth behavior but a fundamentally different mechanism. Ultrathin Au NWs were directly grown from Au seeds anchored on a substrate in an aqueous solution at room temperature.[53] The seeds are far from molten and the size of the emerging NWs is independent of the size of the seeds. The strong ligand in the system prevents deposition of Au on the seed except at the seed–substrate interface. Thus, selective growth at this interface breaks the symmetry of the nanocrystals, thereby leading to unidirectional growth of NWs. The size of the NWs depends on how fast the new NW domain emerges and how fast the ligands passivate its surface.

3.4. Complex T-K Problems

In the above cases, the mechanistic proposals can be clearly assigned as either thermodynamically or kinetically controlled scenarios. As shown in the examples below, sometimes there are mixed effects of thermodynamic and kinetic controls. Thus, the arguments can get entangled. Careful and case-specific analysis is often necessary to elucidate the overall process.

The formation of nanocrystals with thermodynamically controlled facets should be independent of the growth pathways. It is akin to the flowing of water on a tilted floor. The local bumps can easily alter the pathway of flow, but under the influence of the "invisible hands" of the thermodynamics, water is always collected at the lowest basin (the global minimum state). However, if several phenomena are considered together (e.g. defects and facets in the following example), the energy landscape becomes more complex, and it is possible for the system to arrive at the local minimum states (i.e. dents in the floor).

Twinning defects can occur in the nuclei at the early stage of nanocrystal growth.[54] In the theoretic framework of nucleation and growth (Figure 7a),[21e,26a] once the nuclei grow beyond the critical size, there is normally no pathway for them to be completely dissolved (except extensive Ostwald ripening). Thus, the internal defects will always remain. Even when the external facets of the nanocrystals reach equilibrium by dissolution/re-deposition, the overall shape is permanently altered by the internal twinning defects.[55] In other words, the specific pathway directs the system to a local minimum state. Modified Wulff construction can be applied to analyze such twinned nanocrystals.[56]

A contrasting example is the selective growth of single-crystalline Ag NPs by introducing oxidative etching (Figure 10).[57] In the presence of Cl^- and O_2, the nuclei with twinning defects are more prone to etching than those with a single-domain. The latter eventually emerges to give single-crystalline NPs. In a sense, the oxidative etching makes the system more reversible, thereby helping the individual NPs to approach the global minimum state. Here, the thermodynamics exerts its effect at the critical stage of forming the nuclei. At the later stage of growth, the absence

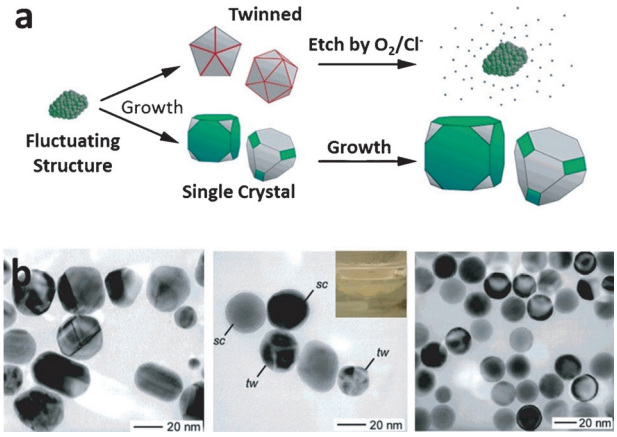

Figure 10. The effects of oxidative etching. a) Schematic representations illustrating the growth process, where the twinned NPs are selectively dissolved by oxidative etching. b) TEM images of the Ag NPs obtained after 10 min (left), 2 h (middle), and 44.1 h (right). Inset: photograph of the reaction mixture at 2 h; it is nearly colorless because most of the Ag NPs are dissolved. Reprinted from Ref. [57] with permission. Copyright 2004 American Chemical Society.

of the pathway, although having no twinning defects is still favorable, would mean that the thermodynamics has no further control over the defects.

In nanocrystals with fivefold twinning defects (decahedra or pentagonal NWs), the presence of defects is unfavorable for the lattice energy, but its presence leads to the maximized formation of (111) facets, which is favorable for the surface energy.[1a,58] It is conceivable that the surface energy would dominate for very small NPs, because of the high percentage of surface atoms. In the case of large nanocrystals, the defect-induced strain becomes intolerable and so the lattice energy would dominate.[7b] However, it is inappropriate to use thermodynamic arguments for analyzing large nanocrystals, because even if the thermodynamics is favorable, it will be too late to induce or remove the defects. The thermodynamic control, if it exists, must occur at a stage when the nanocrystals can still sample over the various forms, more specifically, when some of the nuclei can be re-dissolved before reaching the critical size (Figure 10a), or if small nanocrystals can somehow change their internal structure by "flowing" (Section 3.2.1).

It should be noted that the static states (e.g. the shape of the nanocrystals) are usually insufficient for distinguishing whether thermodynamics or kinetics dominates. For example, spherical NPs can form either because of the isotropic diffusion kinetics (Section 3.3) or because their facets are equally stable (Section 3.2 Figure 5); faceted grains can form either because of the stable facets (Section 3.2) or because of the rapid growth at the unstable facets (Section 3.3.3). Study of the trapped intermediates and in situ investigation of other observables are often necessary to help establish the process.[59]

4. Growth of Hybrid Nanostructures

Over the past few decades, single-component nanostructures have been studied extensively. Recently, the research focus of the field has started to shift towards multicomponent or hybrid nanostructures, that is, structures with at least two domains with different compositions.[60] The additional interface between the domains must be considered for such nanostructures.

4.1. Thermodynamic Analysis

The conformations of double-domain particles can be analyzed as the "wetting" of one material by another. For thermodynamic analysis, only the final state is of importance, while the pathway of domain formation (by flowing or growth) is of less importance.

The simplest case to consider is the merged states of two immiscible liquid droplets (**1** and **3**, Figure 11). The interfacial energies of such droplets in a third immiscible solvent (**2**)

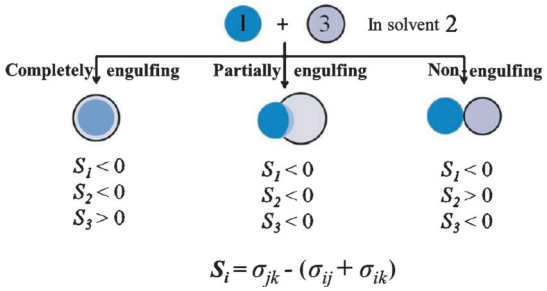

Figure 11. Equilibrium configurations for two immiscible liquid droplets (**1** and **3**) in a third immiscible solvent (**2**). Reprinted from Ref. [61] with permission. Copyright 2013 American Chemical Society.

have previously been investigated.[61] Basically, there are three interfaces (with areas A_{12}, A_{23}, and A_{13}) that have different interfacial energies (σ_{12}, σ_{23}, and σ_{13}). The two-component system seeks to minimize the overall interfacial energy ($A_{12}\sigma_{12}+A_{23}\sigma_{23}+A_{13}\sigma_{13,}$). The situation is akin to a three-party tug-of-war, where the competition between the three terms is complex, but the basic principle is straightforward. Whether one droplet can engulf the other can be predicted on the basis of the spreading coefficients [Figure 11 and Eq. (7)].

$$S_i = \sigma_{jk} - (\sigma_{ij} + \sigma_{ik}) \quad (7)$$

Basically, if droplet **1** "hates" (has poor interactions with) solvent **2** but droplet **3** "likes" both **1** and **2**, then **3** will engulf **1**. On the other hand, if droplet **1** "hates" **3**, then they will form separated domains and maximize their own internal interactions (in the form of spherical domains). Partial encapsulation will result for the intermediate cases.

This analysis can be extended to nanostructures because it is based on geometric considerations. A requirement is that

the interfaces should have uniform properties (ligand density, charges, etc.), so that the interfacial energy is proportional to the interfacial area. Unlike bulk droplets, the interfacial energies of nanostructures cannot be readily measured. However, one can often deduce their trends on the basis of the bonding interactions at the interface, as will be discussed in Sections 4.1.1 and 4.1.2.

Two juxtaposed liquid droplets can flow into the equilibrium configuration, where the total interfacial energy is minimized. When a polymer domain grows on the surface of a solid NP, the NP core cannot adopt different shapes. If the polymer can flow,[62] it would be safe to assume that this particular domain has adopted a lowest energy configuration with respect to the solid domain. In contrast, two-component NPs where both domains are solid can also reach the lowest energy configuration. They are normally synthesized by solution growth of an extra domain on top of an existing solid particle (e.g. growth of silica on Au NPs). As discussed in Section 3.2.1 and Figure 6, the new domain can approach the lowest energy configuration if there is a dissolution/redeposition equilibrium and/or surface diffusion of the growth material, or if the equilibrium structures are obtained in every step during the growth of the new domain.

4.1.1. *Core–Shell NPs*

Encapsulating NPs in inorganic or polymer shells is a popular method for stabilizing NPs in a colloidal solution. The key issue is to establish strong bonding interactions between the core and the shell, so that the interfacial energy can be greatly reduced (Section 2.2).

If the two domains are of the same type (metal–metal, oxide–oxide, etc.), there are often strong bonding interactions between them, which leads to a small interfacial energy. However, it is normally difficult to predict the trend of the interfacial energy. When two nanocrystal domains have an epitaxial relationship, the trend can be easily predicted on the basis of their lattice mismatch. Basically, larger mismatch leads to larger strain and sometimes more defects, which reduce the quality and quantity of the interfacial interactions and result in a higher interfacial energy. The dependence of the growth modes on lattice mismatch has been studied extensively and reviewed.[63] Encapsulation can be easily achieved if the shell has a small lattice mismatch with the core, for example, in Pd@Au,[64] Pd@Pt,[63b] and CdSe@CdS[65] core–shell nanocrystals.

For dissimilar materials, surface modification is often needed to improve the interfacial interactions. For example, silica cannot readily form effective bonds with Au and prefers homogeneous nucleation to yield pure silica NPs. This problem can be solved by introducing ligands that can bond to both materials, for example, one that contains a -SH group for bonding with Au and -COOH or a -$Si(OH)_3$ group for interacting with silica.[66] Similarly, hydrophobic polymers usually do not have strong interactions with NPs, but encapsulation can easily be achieved with the right choice of ligand.[61a] Such a ligand must have a group that can form strong bonds with the core NP (-SH or -NH_2 for Au,[67] -COOH for Fe_2O_3,[68] etc.) and a hydrophobic tail for interacting with the polymer (through hydrophobic interactions, Section 2.1).[69]

A special case of double modification has also been shown to work, where the NPs were coated by a layer of hydrophobic ligands, followed by a layer of amphiphilic PVP. These treatments make the surface of several types of NPs amenable for the growth of polar ZnO.[33] The strong interactions between the NP–ligand, ligand–PVP, and PVP–ZnO layers result in the apparent NP–ZnO interfacial energy, when considered as a whole, being greatly reduced.

It should be noted that the discussion here focuses on the core–shell interface. The external facets or outline of the shell is governed by the thermodynamics and kinetics of the shell growth, as has been discussed in Section 3.

4.1.2. *Janus NPs*

Janus (two-faced) NPs with two juxtaposed domains are often obtained as the intermediate case between complete wetting (full encapsulation) and complete nonwetting.[70] It is normally difficult to deduce from their shape whether they are thermodynamically or kinetically controlled (Section 4.2). An analysis of the complex cases will be presented in Section 4.4.

In one example, we reported the continuous tuning of the Ag domain on spherical Au cores, thereby giving a series of hybrid structures that were assigned as the near-equilibrium configurations (Figure 12).[71] The interfacial energy between any two nanocrystals (e.g. Au and Ag) is usually not considered as tunable, because the nature of the interaction and the lattice mismatch cannot be modified. In our system, however, ligands were embedded in between the Au–Ag layers and their amount can be tuned. A large number of the ligand-induced defects lead to weaker interactions and thus, a higher interfacial energy. Uniform hybrid NPs with core–shell, eccentric, or Janus structures were obtained with high purity.

It is very difficult to propose distinctive kinetic pathways (Figure 13) with a clear underlying trend for these config-

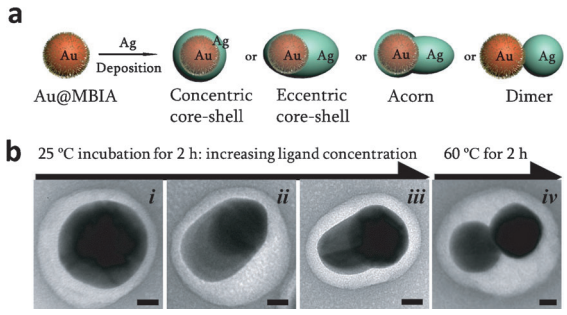

Figure 12. a) Embedding of the ligand 2-mercaptobenzimidazole (MBIA) during the growth of the Ag domain on Au NPs, where the Au–Ag interfacial energy depends on the amount of embedded ligands. b) TEM images of the different types of Au–Ag hybrid NPs: (i) concentric, (ii) eccentric, (iii) acorn, and (iv) heterodimer structures. Polymer encapsulation is used to protect the NPs after their formation. Scale bars are 20 nm. Reprinted from Ref. [71] with permission. Copyright 2012 American Chemical Society.

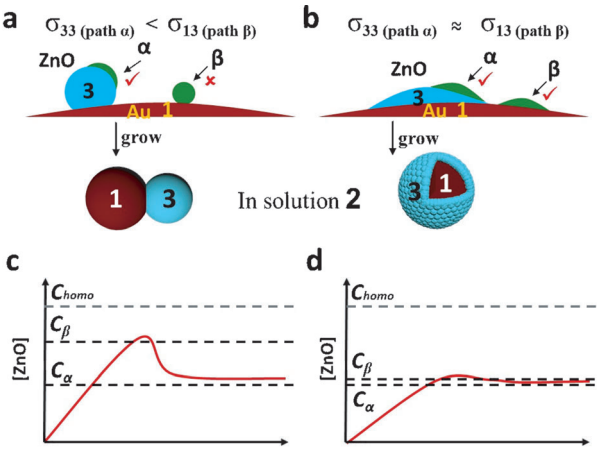

Figure 13. The effects of interfacial energy on the nucleation and growth of ZnO on Au NPs. a,b) Schematic representation illustrating the competitive nucleation pathways when the Au–ZnO interfacial energy is either high (a) or low (b). c,d) Plots of ZnO solubility versus time, highlighting the different growth behavior when the Au–ZnO interfacial energy is high (c) or low (d). Reprinted from Ref. [33] with permission. Copyright 2013 American Chemical Society.

urations. In contrast, the continuous change in the "wetting" of the Ag domain on the Au NPs can be easily explained in the thermodynamically controlled scenario. It is possible that the equilibrium structures are obtained in every step during the growth of the new domain. Basically, the growth of the Ag domain occurred in such a way that the Au–Ag interface was optimized by the "invisible hands" of the thermodynamics. Admittedly, more experiments are imperative to make a clearer distinction between the thermodynamic and kinetic effects.

4.2. Kinetic Analysis

In a thermodynamically controlled scenario, the configuration of the hybrid nanostructures (core–shell, eccentric, or Janus) is independent of the growth pathways. Nevertheless, it is still important to understand how the kinetically controlled scenarios are avoided (by kinetic analysis), that is, what is the course of action that allows the growth material to sample over the various forms. For kinetically controlled systems, it is crucially important to know the key process and the nature of the activation barrier.

Here, we focus on the choice of the hybrid configuration, not the general control of the growth process. The latter can determine, for example, the extent of the homogeneous nucleation and the amount of material in the shell, which are the preconditions for the choice of the structural configuration.

The fluidity of polymer domains or shells can be easily adjusted to design pathways. The glass transition temperature (T_g) of a polymer depends on its chemical composition and the degree of polymerization, cross-linking, and swelling. To render the polymer liquid-like, for example, one can raise the temperature over the T_g or greatly reduce the T_g by swelling. A uniform polymer shell can be created when it is highly swollen by a good solvent, for example, *N*,*N*-dimethylformamide (DMF) for polystyrene-*block*-poly(acrylic acid) (PS-*b*-PAA).[61a] The fast addition of water can then extract the DMF, which causes deswelling of the PS domains. As a result, the PS becomes glassy with a low fluidity, trapping the core–shell nanostructures in kinetically stable states.[72] Similarly, chemical cross-linking can also be used to this end.[67b,73]

In typical core–shell NPs, the shells are not formed instantaneously, but are sequentially built up by solution deposition. Thus, there is a fundamental similarity between different systems in how the free atoms/molecules join with each other and with the cores (i.e. seeds). In contrast to Section 3.3.1, the seeds here have a different chemical composition from the growth material. Thus, the growth must be described by a modified nucleation and growth model as follows.

For example, the growth of the ZnO domain on the ligand-modified Au NPs (Figure 13)[33] is only possible when the interfacial energies are suitable. That is, the thermodynamics must allow it. More specifically, the heterogeneous nucleation of ZnO on the Au surface (path β) must be more favorable than the homogeneous nucleation, otherwise the latter process will dominate. On the other hand, path β is always less favorable than the heterogeneous ZnO nucleation on the ZnO surface (path α), because there is essentially no interfacial energy between two domains of the same material. From the kinetics perspective, these requirements constitute the "activation" barriers for the formation of a newly added domain, where the relative height of the barriers depends on the interfacial energy between the new domain and the underlying surface. Figure 13c presents the basic concept that the oversaturation of the growth material must reach certain levels during the growth before these pathways become allowed.

From these considerations, the build-up of ZnO in solution would reach such a level that ZnO would first form a small domain on the Au NP. Once this happens, the subsequent deposition of ZnO would occur more favorably on the existing ZnO domain than on a fresh location of the same Au NP. This typically leads to a single ZnO domain per each Au NP. On the other hand, if the ZnO–Au interfacial energy can be greatly reduced by using appropriate ligands/surfactants, the threshold for path β would then approach that for path α (Figure 13b). When this difference is small enough, random fluctuation of the concentration or local build-up of ZnO would be sufficient to give new nucleation sites on the Au surface, thereby leading to multiple nucleation sites and eventually a merged shell.[74]

In this model, the rate of deposition is conceivably the key factor. At one extreme, if the rate is so slow that the choice between paths α and β is always true, then the most favorable configuration would be obtained in every step and the thermodynamics would dominate. At the other extreme, if the deposition is so rapid that paths α and β are equally probable, a metastable core–shell structure might be obtained even if the interfacial energy is unfavorable. A huge oversaturation may allow both pathways and/or make the redissolution process negligible, but it should also lead to extensive homogeneous nucleation.

The growth conditions can be designed to achieve rational pathways. For example, small Au NPs can be decorated on the surface of silica[75] (or $NaYF_4$)[76] NPs. By using them as the seeds, Au deposition would lead to a rough but complete metal shell (Figure 14a). Without these initial seeds, a very

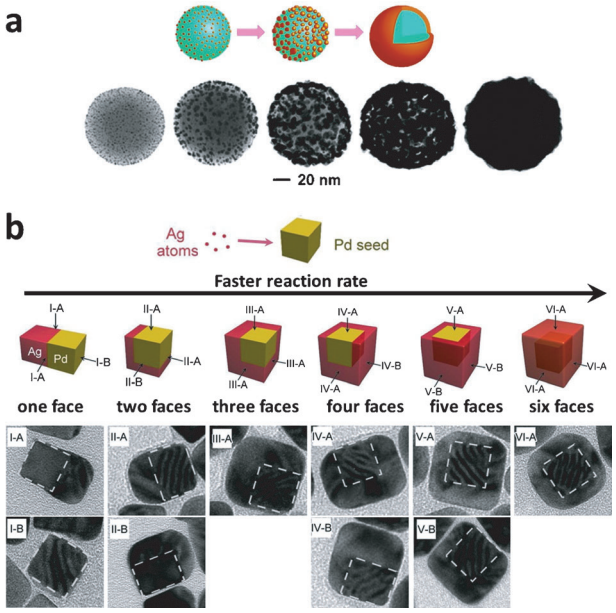

Figure 14. a) Schematic representation and representative TEM images illustrating the formation of the merged Au nanoshell on the silica NPs by first decorating them with seeds. b) Schematic representations and representative TEM images (viewing from different directions) illustrating the kinetically controlled overgrowth of Ag on the Pd cubes. Reprinted and modified from Ref. [75e,f,77c] with permission. Copyright 2007 American Chemical Society, 2004 Adenine Press, and 2012 American Chemical Society.

different result would be obtained (rarely any heterogeneous nucleation), because a newly formed Au domain would have a high silica–Au interfacial energy. The presence of the seeds permits numerous nucleation sites on each silica NP, eventually giving a merged shell that is thermodynamically unfavorable. If the Au shell could flow, it would contract into a single domain to reduce the Au–silica interface.

Xia and co-workers demonstrated the versatile synthetic control of bimetallic NPs by modulating the rate of the chemical reaction that produces the growth materials.[77] As shown in Figure 14b, Ag was selectively grown on 1 to 6 faces of the Pd cubes, whereby an increasing number of the faces were coated with the increasing reaction rate. It was proposed that the faster reaction caused more faces to become the "active growth sites" (compare with Section 4.1.2), where the initially coated Ag layer facilitated the subsequent deposition, whereas the rest of the faces remained inactive because of the lattice mismatch between Pd and Ag.[77c]

4.3. Templated Growth

In essence, the templated growth of nanocrystals can be viewed as the growth of the crystalline domain on the surface of the template, thus making it a two-component system.[78] Should the template–nanocrystal interfacial energy be high, the formation of the interface would be both kinetically and thermodynamically unfavorable, thereby leading to the homogeneous nucleation of free nanocrystals in the solution, unaffected by the template. Thus, for all known cases of templated growth, the interfacial energy must be low enough to allow conformal coating or at least multiple nucleation sites that can eventually lead to a merged domain. As discussed in Section 4.1 and Figure 11, there are three interfaces (template–solvent, template–nanocrystal, and nanocrystal–solvent). Therefore, the shape of the nanocrystals depends not only on the shape of the template but also on the interfacial energies.

Templated growth has been widely postulated for many anisotropic nanocrystals, particularly nanorods and NWs.[39c,78b,79] Unfortunately, the detailed processes are difficult to characterize and have so far remained elusive. There is a battery of questions to be asked. First and foremost, the template–nanocrystal interface is of pivotal importance, but it is often poorly understood, for example, what the exact interactions are between the CTAB head group and the Au surface.[80] With more insight, one may hopefully be able to tune the interface, expand the scope of the templates, and improve the synthetic control. Second, the diffusion of the growth materials is a major problem for the growth of nanocrystals inside templates (e.g. cylindrical micelles; Figure 15b).[78b] Should nucleation occur near the opening of the

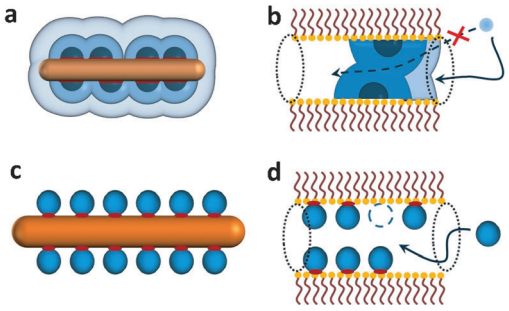

Figure 15. a,b) The templated growth of nanocrystals and c,d) the templated assembly of NPs. The template–NP interfaces are highlighted in red. The diffusion of the growth material or NP is not a limiting factor for (a) and (c); but the random nucleation or adsorption of NPs inside a template can easily cause problems.

micelle, the newly generated nanocrystal domain will block the supply of the growth material. Last, the complex interplay between the template and the emerging nanocrystal has not been fully established. For example, the assembly of the CTAB micelles may occur simultaneously as a result of the growth of the Au nanorods. The dynamic motion of the CTAB molecules in the cylindrical micelles may generate porosity in the micellar wall and, thus, allow the diffusion of the growth materials across it.

The colloidal growth of ultrathin NWs,[39a,50] often proposed to be the result of templated growth, is very different from the growth of most other nanocrystals. The scope of the applicable templates is extremely narrow. The width of the ultrathin NWs is unusually monodisperse and rarely tunable.[50,81] What stops their lateral growth when a certain width is reached? Growing long NWs from short NWs has not been demonstrated. The NWs have not been shown to grow from a bulk crystal surface. More insights into the templated growth may help elucidate these mysteries and improve the synthetic design.

4.4. Complex T-K Problems

When there are multiple components and multiple processes in a system, it is conceivable that its energy landscape is significantly more complex than that of the single-component systems. In the deposition of shell materials on core NPs, for example, one needs to consider the coordination and dissociation of ligands on the cores, the nucleation and growth of the shell materials, the core–shell configuration, and the ligand coordination to the shells. Given the different processes and their possible interplay, mixed T-K arguments are rather common in such systems.

A good example is the growth of conformal silica shells on Au nanorods.[82] When the shells are very thin, the overall shape resembles that of the initial Au nanorods. When the shells grow thick, however, the silica outline gradually approaches a spherical shape, which suggests a diminishing structural influence of the internal core (Figure 16a–c). We can analyze the T-K problem by comparing the transverse growth (silica thickness of α) to the longitudinal growth (silica thickness of β). At one extreme, when $\alpha = \beta$, the uniform silica shells would suggest indiscriminative deposition (likely because the deposition is irreversible). Although the overall shape does appear to be rounder, it is solely because the equal increase in the length and width leads to a decreased aspect ratio. Another evaluating characteristic is that the lateral surface should remain parallel to the side surface of the Au nanorods (as in straight cylinders), not curved like that of ellipsoids. Such a growth can then be assigned as kinetically controlled. At the other extreme, when the silica outline is exactly a sphere ($\alpha > \beta$), the growth is clearly thermodynamically controlled (Section 3.2). Intermediate cases between the two extremes are likely, as the increase in the shell thickness is gradual and the reversible dissolution during the silica deposition is usually not extensive.

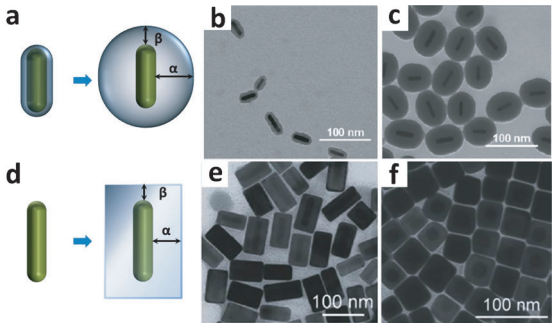

Figure 16. Schematic representation and TEM images illustrating the formation of amorphous (a–c) and faceted shells (d–f) on anisotropic seeds. The growth can be judged by the extent of growth at the different directions when the shell is amorphous (a), or at the eqivalent facets when the shell is faceted (d). b,c) TEM images of the silica-coated Au nanorods, with thin and thick silica shells, respectively. e,f) Side and vertical views of the Ag-coated Au nanorods, where the Ag shells are faceted. Reprinted from Ref. [82, 85] with permission. Copyright 2011 American Chemical Society, 2012 Royal Society of Chemistry.

This method of analysis may be applied to other core–shell systems. Ideally, the shell should be amorphous or without selective facets, for example, the coating of polymer shells on Ag nanocubes[83] and Au nanorods,[84] and the heteroepitaxial growth of Pd on Pt nanocubes (control experiments without the seeds gave nonspecific NPs).[63b] In a different case, the formation of cuboidal Ag shells on highly anisotropic Au nanorods[85] requires unequal growth of the Ag(100) facets, which suggests an underlying thermodynamic influence (Figure 16d–f).

Assigning the thermodynamically controlled configuration to solid shells may seem difficult to comprehend. Although the effects of the "invisible hands" of thermodynamics can be recognized, the exact underlying pathways are still unclear. A possible explanation is that the reversible deposition and dissolution processes as well as a subtle difference in the rates may help guide the overall shape towards a form with the lowest surface energy, even though each monomer species does not "know" the overall shape. In this aspect, these cases are similar to the control of spherical shape in Section 3.2.1 and the control of configuration of the hybrid Ag–Au NPs in Section 4.1.2 (Figure 12).

In the analyses in Section 4, the surface properties of the cores are considered as uniform, in particular the ligand layer. The situation becomes more complex if there are multiple ligands that form segregated patches on the core. The competition between hydrophobic and hydrophilic ligands has been employed to adjust the coating of PS-*b*-PAA on Au NPs, where the polymer only attached to areas covered with the hydrophobic ligands.[86] The ratio of polymer coverage per NP can be tuned by adjusting the ratio of the two ligands. The sequence of ligand introduction was shown to affect the final polymer–Au configuration, thus suggesting that ligand kinetics play a pivotal role. However, the details of ligand kinetics have yet to be established because of the limits of the characterization methods.

5. Aggregation of Nanoparticles

Here, "aggregation" is defined as the direct touching of NPs or their surface ligands, whereas "coalescence" is defined as the merging of the NP domains with extensive cohesive interactions (similar to those within the NPs) at their junction. In the former case, we are often interested in why the NPs want to stay in contact with each other (the thermodynamic driving force) and how the NPs find each other in a colloidal solution (the kinetic pathways). In the case of coalescence, we

are interested in the energetic benefit of merging and the pathways that allow the transfer of materials.[87]

5.1. Thermodynamic Analysis

The aggregation of NPs is a precondition for their coalescence. In the following, the coalescence is treated as a separate phenomenon in our analysis. If the two processes are considered together, the most stable state of a collection of colloidal NPs would be a single coalesced sphere, which hardly ever happens. When considering the coalesced sphere as the final state, all the NPs in any solution can be defined as unstable. It is also important to note that being the later process, partial coalescence can render a collision process irreversible, but it exerts no control over the NPs until they make contact.

With a few exceptions under special conditions,[87b,88] the coalescence of nanostructures is not extensive.[89] The surface ligands usually prevent direct contact and bonding between two neighboring NPs. Without coalescence, the contact area between the spherical NPs would be only a small percentage of the overall NPs. Thus, the driving force for reducing the NP–solvent interfacial energy would be far less than that of the complete coalescence.

In a sense, the aggregation of NPs can be likened to the aggregation of atoms or ions to form solids.[89a,c,90] When NaCl crystals are formed in a solution, for example, the stabilization energy of both the starting and the ending states should be considered. That is, the entropy (the freedom of the ions as opposed to their orderliness in a crystal lattice) and solvation energy (the favorable interactions with the solvent molecules) of the free ions compete with the lattice energy of the NaCl crystal in governing the dissolution/crystallization processes.

Similarly, only considering the interactions among the NPs in the aggregated state would be insufficient. For a free NP in an aqueous solution, for example, more favorable (negative) solvation energy is expected when the NP has more surface charges, more groups with hydrogen-bonding capability, etc. Hence, it is the energetic difference between the free colloidal form and the aggregated state that determines the driving force.[28] To prevent aggregation of the NPs, one can choose ligands that have a strong interaction with the solvent and/or those that interact more weakly with each other (when between two opposing NPs). Roughly speaking, the NP–NP interactions should be stronger than the solvent–NP interactions for aggregation to occur.

When more than two NPs aggregate, one needs to compare the stability of the different potential forms, such as the free colloidal form, the linear chains, the loose network of globular clusters, and the densely packed globular clusters (Figure 17). The number of junctions per NP increases in the sequence given. The interactions between the neighboring NPs at the junction can be likened to a chemical "bond", whose energy to a large extent depends on the ligand layer. If the formation of one junction is favorable (that is, the NPs want to aggregate), the formation of multiple junctions would usually be more favorable. To maximize the number of junctions, the most stable state would be a near-globular cluster made of close-packed NPs (Section 5.4). Thus, the shape of NP aggregates can be analyzed by the methods in Section 3.2. In other words, all of the other forms, if existing, should be merely metastable. These arguments are based on the assumption that the charge or dipole interaction between the NPs is not the dominant term. Otherwise, the situation would be more complex (Section 5.5).

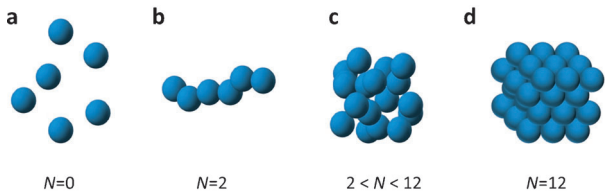

Figure 17. Possible states of NP aggregation: a) the unaggregated state; b) the chain aggregate; c) the loose globular aggregate; and d) the supercrystal. The average number of junctions per NP (N) increases in this order.

5.2. Kinetic Analysis

Having a driving force to aggregate does not mean that the NPs can actually do so. The NPs need to find each other by random collision, then overcome the barrier (e.g. charge repulsion), before establishing effective "bonding" interactions. The size distribution of the resulting clusters is critically dependent on how the NPs find each other by random collision. This process can be likened to the polymerization modes of organic monomers (Figure 18a), namely the step-growth and the chain-growth mode.[91] Basically, in the former mode, all the monomers and oligomers have a similar tendency (probability of effective collision) towards aggregation, whereas in the latter mode, a few species (e.g. radicals or initiators) can undergo extensive polymerization but a signifi-

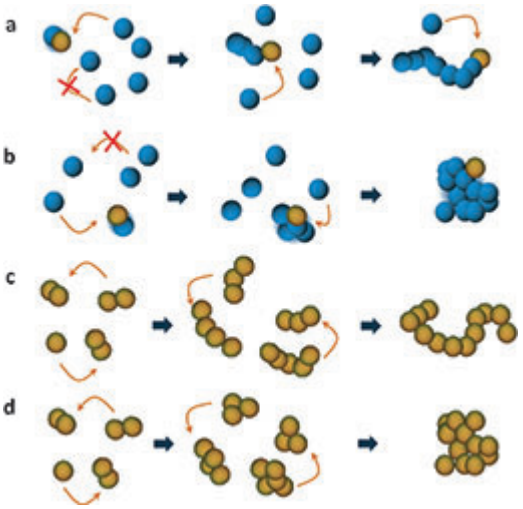

Figure 18. Categories of aggregation. The shape of the aggregates may be either chainlike (a,c) or globular (b,d) and the aggregation process may follow either the chain growth mode (a,b), where only a few species are "active" (marked in yellow); or the step-growth mode (c,d), where the different-sized aggregates are equally active.

cant amount of the monomers remain intact. On the other hand, according to the shape of the aggregates, the aggregation can be categorized as globular or chain aggregation. Thus, there are four categories, as illustrated in Figure 18.

At first sight, the aggregation of two monomeric NPs should be no different from that of two NP clusters. Thus, the overall process should be similar to the step-growth polymerization of organic monomers[92] (see Section 5.4 for a contrasting example). The similarity also originates from the fact that any cluster (oligomer) must be formed sequentially through the two-party collision of monomers and smaller clusters, because three-party collision would be statistically improbable. When a collection of NPs start to aggregate, the monomers are quickly consumed, thereby giving rise to dimers and then trimers,[92b] which further aggregate with each other to give larger clusters. The process is dominated in the later stages by the aggregation of large clusters. Such a kinetic pathway typically leads to clusters with a large size distribution. The exact process has been nicely demonstrated in the end-to-end aggregation of Au nanorods,[92a] which were selectively functionalized with polystyrene (PS) on both ends.

Considering the charge repulsion between NPs, however, the aggregation of monomers (the effective collisions) would be significantly more probable than that of the large clusters. The potential energy of the repulsive interaction between two charged spherical particles, V_{elec}, can be expressed as Equation (8), where $L_e = \kappa^{-1}$ is the Debye screening length, calculated from the dielectric constant ε of the medium, the Boltzmann constant k, the temperature T, the elementary charge e, and the ionic strength I of the electrolyte [Eq. (9)]. a_i is the respective particle radii, h_m is the separation distance between the colliding particles, and ϕ_i is the respective surface potentials of the particles. Assuming the same surface charge density (a result of the surface ligand density), the charge repulsion is stronger when the NPs or clusters become larger.[93]

$$V_{elec} = 4\pi\varepsilon\psi_1\psi_2 \frac{a_1 a_2}{a_1 + a_2} \ln\left(1 + e^{h_m/L_e}\right) \quad (8)$$

$$L_e = \kappa^{-1} = \left(\frac{\varepsilon kT}{2el}\right)^{1/2} \quad (9)$$

When Au nanorods with PS covering both ends are used,[92a,94] it is conceivable that the sizeable PS domains (about 4 nm) would make the end-to-end charge repulsion less influential. For ligand-functionalized Au NPs, in contrast, charge repulsion is probably the reason for the deviation from the step-growth kinetics.[92b]

Our group carried out a case study on the effects of charge repulsion using the "cross-coupling" of different NPs as a platform. An excess of the citrate-stabilized Au NPs (B-NPs) was used to react with thiol-modified Au NPs (A-NPs) (Figure 19).[95] Given the strong Au–S bonds between the NPs, one would expect the excess B-NPs to form a close-packed shell surrounding the A-NPs. This was not observed. Instead, the result of the aggregation (AB, AB_2, AB_3, or AB_4 clusters) was dependent on the salt concentration, which plays an important role in shielding the charge repulsion between the B-NPs [Eqs. (8) and (9)]. We showed that charge repulsion is the dominant factor in the kinetic barrier of the aggregation process (Figure 11). Thus, the long-range charge repulsion determined the structure of the product (AB_n) before the NPs even make contact with each other. Once they make contact, the short-range bonding interactions (Au–S bonding, van der Waals interaction, etc.) dominate, thereby preventing their separation. Although products with increasing coordination numbers would be more energetically favorable ($AB_4 > AB_3 > AB_2 > AB$), the kinetic barrier of the system prevented the products from sampling over the alternative forms. In other words, the processes were kinetically controlled.

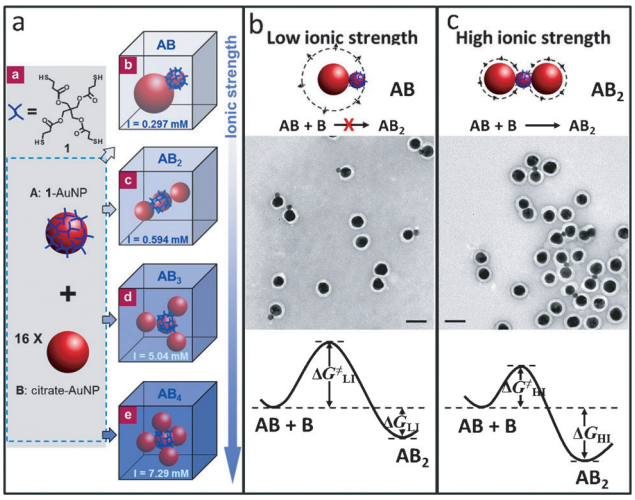

Figure 19. a) Syntheses of AB, AB_2, AB_3, and AB_4 nanoclusters by tuning the charge repulsion between the B-NPs. The type A Au NPs are fully covered with thiol groups, and 16 equivalents of the type B Au NPs are used for their coupling. b) At low ionic strength, the strong repulsion between the type B NPs limits only one type B NP per each type A NP. c) At a higher ionic strength, AB_2 becomes allowed, but AB_3 is still unfavorable. Polymer encapsulation is used to protect the product clusters after their formation. All scale bars are 50 nm. Reprinted from Ref. [95] with permission. Copyright 2010 Nature Publishing Group.

A distinctively different mode of aggregation was observed when a special type of monomers was used, namely the Au@PSPAA core–shell NPs, where the Au NPs were fully encapsulated in PS-*b*-PAA shells. Treatment with acid results in the formation of ultralong chains of the Au NPs. The surprising observation was that a significant amount of the monomers still remained when some monomers had aggregated extensively into long chains. This result is drastically different from the typical products of the step-growth kinetics, but similar to that of the chain growth polymerization. Pure PS-*b*-PAA spherical micelles (without the embedded AuNP) are known to transform into cylindrical micelles under acidic conditions.[96] Thus, the behavior of the polymer played the dominant role in the aggregation, favoring the formation of the very long NP chains and confining their transverse width. The underlying reason for the sustained chain propagation has not been established, although we postulate that the disorganized PS-*b*-PAA

domains (Section 6.2) at the growing end may lead to an "activated" site that promotes continual aggregation.

Brownian motion is an important kinetic factor. It originates from the random collision of solvent molecules with NPs. At any instant, the imbalance of the collision leads to a net force. Larger NPs have smaller imbalances and, thus, less energetic Brownian motion. This situation can be likened to the rocking of small and large boats in the ocean. Higher temperature leads to a larger kinetic energy of the solvent molecules, and thus more energetic Brownian motion of the NPs. As Brownian motion is random, it does not provide any thermodynamic driving force, but it can help overcome the barriers in both forming and dissociating the aggregates.

In summary, when NP aggregation is thermodynamically controlled, the main competition is between the stabilization energy of the free colloidal form (solvation energy, entropy, charge repulsion, etc.) and that of the aggregated forms (attractive interactions between the NPs, hydrophobic interactions, etc.). When charge repulsion is the main kinetic barrier that prevents the effective collision of certain NPs, the main competition is between the kinetic energy of the NPs and the height of such a barrier. A strong surface charge may render the NPs either thermodynamically or kinetically stable in the solution. In the former scenario, the NPs want to dissociate even if they are aggregated, while in the latter, the NPs want to aggregate but strong repulsion prevents effective collision. The main competition during the dissociation of NPs is between the kinetic energy of the NPs within the cluster and the attractive interactions between them. In experiments, NPs that are precipitated in one solvent can sometimes be re-dissolved in another, because the improved solvation energy of the surface ligands leads to a more favorable thermodynamic driving force. Alternatively, sonication can generate a strong sheer force in a solution, thereby providing additional kinetic energy for dissociating the NPs in a cluster.

5.3. Templated NP Assembly

There are quite a large number of reports on the orderly assembly of NPs by adsorbing them on the surface of colloidal templates such as DNA constructs,[97] soft micelles, other types of nanostructures,[98] or bulk surfaces.[39c] These systems have been reviewed extensively,[78a,89d,99] and thus will not be discussed in detail here. The situation is somewhat similar to the templated growth in Section 4.3, except that NPs are adsorbed instead of atoms (Figure 15). For the process to be thermodynamically favorable, the template–NP interactions should be stronger than the template–solvent and NP–solvent interactions. Typically, the NPs do not adsorb on top of existing NPs and prefer a fresh location of the template (Figure 15d), likely as a result of the charge repulsion between them. Using a similar argument, the relatively uniform separation between the NPs on a template surface can also be explained. In these systems, the surface of the template is of critical importance, including its surface chemistry, charge density, and solvation energy. These properties are highly case-specific but difficult to characterize.

5.4. Supercrystals of NPs

Extensive aggregation of NPs can sometimes lead to orderly 2D arrays or 3D supercrystals.[100] The general principles and specific phenomena relating to the supercrystals of NPs have been nicely reviewed recently.[28] In this category, the main concern is the crystalline order, that is, the choice between the loose network of globular clusters (analogous to an amorphous state) and densely packed globular clusters (a crystalline state). Considering the unlikelihood of forming perfect crystals by random collision during the formation of the supercrystals, the individual NPs must have sampled over various locations before settling at the most stable position. Hence, the overall process (not the size/facet, compare to Section 3.3) is generally considered as thermodynamically controlled.

Several types of packing order in supercrystals of NPs have been reported. Small clusters (< 20 NPs) have been obtained with icosahedron-based structures, that is, they were "building either en route to or on top of an icosahedron" (Figure 20a,b).[101] The structures are similar to the Lennard–Jones series of atomic clusters.[1a,102] In contrast, large clusters usually have close-packed structures such as an fcc lattice (Figure 20c,d).[103] The basic units used for making supercrystals are typically spherical NPs, but uniform nanorods

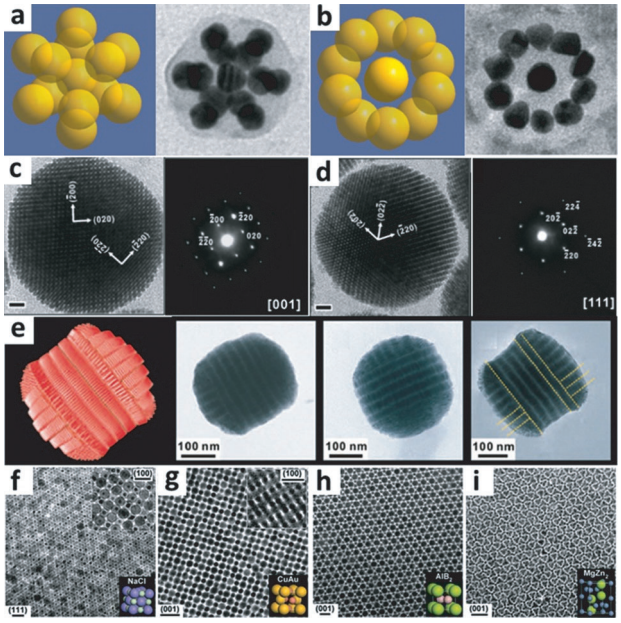

Figure 20. a,b) Schemetic representations and TEM images of icosahedral superparticles made of Au NPs, showing the clusters from different projection directions; c,d) TEM images and SAED patterns of superparticles made of the Fe_3O_4 NPs that are capped with hydrophobic ligand, viewed along the [001] zone axis (c) and the [011] zone axis (d). The scale bars are 20 nm. e) Schemetic representation and TEM images of the double-domed cylinder supercrystals assembled from CdSe–CdS nanorods; f,g) binary supercrystals assembled from 13.4 nm g-Fe_2O_3 and 5.0 nm Au NPs (f); 7.6 nm PbSe and 5.0 nm Au NPs (g); 6.7 nm PbS and 3.0 nm Pd NPs (h); and 6.2 nm PbSe and 3.0 nm Pd NPs (i). Reprinted from Refs. [101a, 103e, 104b, 105b], respectively, with permission. Copyright 2012 AAAS, 2007, 2013 American Chemical Society, and 2006 Nature Publishing Group.

have also been shown to work, with formation of multidomain superstructures (Figure 20e).[104] Binary supercrystals have been synthesized by using NPs with opposite charges (Figure 20f–i).[105]

From the thermodynamic perspective, a supercrystal of NPs has less favorable entropy and solvation energy but a larger number of NP–NP junctions than an amorphous cluster. Under the conditions that the NPs want to aggregate, the driving force is to minimize the number of NPs sitting on the surface and to maximize the number of NP–NP interactions, a situation similar to that discussed in Section 2.2. There are at least two scenarios to achieve NPs with a well-ordered packing: 1) the NP aggregation is reversible, so that the erroneous additions can be corrected by repetitive association and dissociation; and/or 2) there is structural fluidity in the cluster, where NPs can slide across each other and adjust their positions without dissociating. Well-ordered supercrystals are typically prepared from NPs that are coated with either hydrophobic ligands[32c,103a,f,104b] or DNA.[106] The hydrophobic NPs dislike polar solvents and weakly interact with each other. As such, the solvophobic interactions provide a strong driving force for aggregation, but the NP–NP interactions are weak enough to allow structural rearrangement. The DNA-functionalized NPs are highly charged and the attractive interactions between them can be readily adjusted by tuning the number of base pairs in the complementary section. For the other types of NPs, the reversibility and structural fluidity can be compromised if there is a sufficient amount of strong interactions, for example, when the NPs can be partially coalesced, when the ligands can covalently bridge them, or when the opposing ligand layers can strongly interact (e.g. through hydrogen bonding).

The concept of facets can be applied to supercrystals (compare with Section 3.2, Figure 5), and the modified Wulff construction can be used for analyzing the multidomain supercrystals.[104b] Basically, the stability of a NP sitting in a facet depends on the number of "bonds" (NP–NP junctions) it has with its neighbors. Thus, the different facets would have different NP densities, thereby giving rise to different "surface energies". It is important to note that the "surface energy" here is defined as the lack of NP–NP "bonds" at the surface of the supercrystal [the same definition applies to Eqs. (4)–(6)]. Although the capping ligands on the NPs can affect the NP–NP "bonds", they are too small to directly influence the facet stability of the supercrystal, unlike the case of normal crystals where the ligands are larger than the atoms (Section 3.1).

The kinetic pathway to the formation of supercrystals can also be compared and contrasted to that of normal crystal growth (Section 3.3.1). Similar to the latter, a larger cluster of NPs has less "surface energy" and is thus more stable. More specifically, for a newly added NP, it forms 3 NP–NP junctions ("bonds") when added to a tetrahedron, thereby giving a trigonal bipyramid, but 5–8 "bonds" when added to the step on a (111) facet. Thus, forming the trigonal bipyramid would be more difficult, but dissolving it would be comparatively easier [Eq. (2)]. On the other hand, for the nucleation barrier to exist, the initial small clusters should be less stable than the solubilized monomers.[28] In crystal growth, there is a drastic change in the environment of an atom/ion in the solubilized form on switching to an adsorbed state on the surface of a nucleus, but such a change should be much smaller for a colloidal NP, which is already a solid phase from the start.[28] Hence, the energy barrier for nucleation during the assembly of supercrystals should be much smaller. A consequence of this argument is that the absence of the energy barrier for nucleation would invalidate the concept of "critical size" during the formation of NP clusters. A possible counter argument of this proposal is that, although the energy barrier for the nucleation of NPs is much smaller than that of atoms, the kinetic energy of NPs (their Brownian motion) is also much smaller.

Without the energy barrier for nucleation, the monomers will become depleted because they are not being regenerated by the dissociation of the initial clusters. With few monomers remaining, the later stage of aggregation would be dominated by cluster collision, as opposed to monomer addition. This would be similar to the step-growth mode and lead to a broad size distribution (Section 5.2). Hence, there is a challenge to provide additional rationales in cases where supercrystals with narrow size distributions are obtained. One proposal is that the diffusion of NPs may be the limiting factor; the bottleneck would be more severe for building larger clusters, because a larger number of NPs are required (assuming growth by monomer addition).[28] This situation is similar to that of the "size-distribution-focusing" effects (Section 3.3.1).[18,107] Another hypothesis is that the charge repulsion between the clusters is responsible for the size-limiting effect of the supercrystals.[108] As the clusters grow in size, the stronger repulsion between them [Eq. (8)] eventually brings the aggregation to a halt.

There is another difference in the growth kinetics. In crystal growth, there is usually a steady supply of growth material by chemical reactions. One can easily adjust the rate of the chemical reaction so that the oversaturation of the growth material can be maintained at a low level to suppress homogeneous nucleation. In growing supercrystals, however, all the growth materials (namely NPs) are typically present at the beginning. Thus, controlling the nucleation and growth would be significantly more challenging. Sequential addition of NPs has so far not been fully exploited as a means to control the growth kinetics.

Thus far, the discussion on the growth kinetics has focused on how the NPs find each other through random collision, which should not be confused with the structural rearrangement. The aggregation of clusters (as opposed to NPs) is rather common in the step-growth mode. Without the process of coalescence, the voids/gaps in the product cluster and the misalignment between the domains cannot be corrected, thereby leading to amorphous clusters with irregular shapes. Considering the basic step of coalescing two spherical clusters, for example, the final shape of the aggregate may appear as two juxtaposed spheres, a partially merged dumbbell, or a completely coalesced sphere, depending on the degree of coalescence. Unless the structural rearrangement is efficient, further aggregation may lock the overall cluster, thereby giving imperfections. With these considerations, the spherical shape of the typical supercrystals in the literature is likely

a result of growth by monomer addition with an association/dissociation dynamic or structural fluidity of the supercrystals.

5.5. Spontaneous Aggregation of NPs into Chains

There are numerous reports on the assembly of NPs into chains.[109] The formation of chains requires the selective bonding at only two diametric directions, which is surprising because most of NPs have more than two equivalent directions or facets. Moreover, the assembly of chains with only two junctions per NP is apparently less favorable than the assembly of globules with multiple junctions (Figure 17). To understand the choice between the assembly of chains and globules one needs to identify the key factor favoring the chain structure, more specifically, to determine whether it is thermodynamically stable or kinetically favored.

Many mechanistic proposals have been put forward. The most straightforward explanation is that the surface ligands may arrange in such ways that only two diametric ends of the NPs are different, thus predisposing the NPs for selective aggregation. Such ligand arrangements are conceivable, for example, CTAB molecules can remain on the side of Au nanorods while those on the ends are exchanged,[110] and the ordered coassembly of hydrophilic and hydrophobic ligands on spherical NPs could give concentric rings of ligands, thus exposing two diametric "whirlpools".[111] As such, among the many possible configurations of random collision, the assembly of the NPs into chains could be the most favorable one. However, studying the arrangement of ligands on NPs is not trivial. Strong evidence has been obtained in only a few systems. For example, PS domains have been observed on the two diametric ends of Au nanorods,[92a] and ripples of ligands were observed by scanning tunneling microscopy (STM).[111b] It should be noted that the observation of chain assembly in itself is not sufficient proof for the ligand organization (or any particular mechanism), unless the alternative possibilities can be ruled out. For example, charge repulsion between the Au nanorods may lead to a higher activation barrier for their side-to-side collision, thus favoring the end-to-end assembly as the kinetically controlled product.

Another mechanism favoring chain assembly could be through the interaction of dipoles. If it is the dominant factor, the formation of a chain assembly would be both thermodynamically and kinetically favored. A clear cut example is the assembly of magnetic NPs in the presence of an external magnetic field, where the NPs could form very long chains with few errors.[112] On the other hand, electric dipoles can be invoked to explain the assembly of nonmagnetic NPs into chains,[109a,113] although the origin and strength of such dipoles have yet to be fully established. For a semiconductor NP, the balance of the total charge within the NP requires one facet to be cation-rich and the opposing one anion-rich, thereby leading to a net dipole[114] (presumably in multiple equivalent directions). Suppose that the assembly of a chain is thermodynamically favorable as a result of dipole interactions, the potential of the electric dipole should be strong enough to compensate for the lack of NP–NP interactions. There are 2 NP-NP junctions per NP in the chain assembly versus 12 junctions in the globular assembly (Figure 17). On the other hand, if the chain assembly is kinetically favored, it is of interest to identify the nature of the kinetic barrier (charge or dipole repulsion, etc.) so as to prevent erroneous addition that would lead to the globular assembly.

Charge repulsion by itself can also lead to the aggregation of NPs into chains. Wang and co-workers were the first to point out that a NP approaching the end of an existing chain (the end-on aggregation) would encounter less charge repulsion than one approaching from the side.[92b,115] There are two possible scenarios: 1) the electric repulsion potential may destabilize the globular assembly sufficiently to cancel out the excess of NP–NP "bonds" therein, thus making the chain assembly the thermodynamically stable state (Figure 21);[115b]

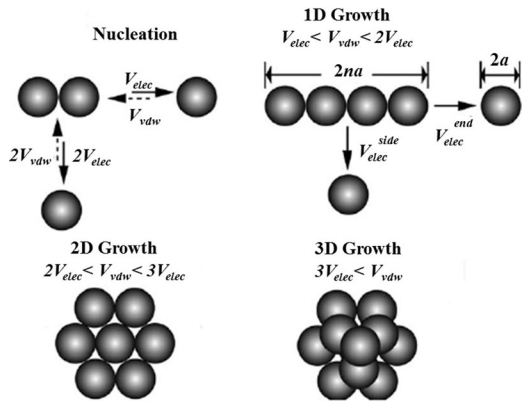

Figure 21. The role of charge repulsion in aggregation. The repulsion experienced by an incoming NP towards a cluster is different from the different directions, so is the van der Waals interaction. The boundary conditions can be determined as illustrated. Reprinted from Ref. [115b] with permission. Copyright 2008 Wiley-VCH.

2) the electric potential may merely facilitate the pathway of chain assembly, but the globular assembly is still the most stable state.[93a] It is important to note that the interactions involved in the process have different effective distances. In general, charge repulsion is long-ranged, whereas chemical bonding and van der Waals interactions are short-ranged. For scenario 1, all interactions should be included because all potential energy terms are integrated as two NPs approach and then make contact. For scenario 2, however, the transition state is of crucial importance. If the NPs are highly separated at the transition state, the short-ranged interactions cannot exert their influence.

To distinguish the two scenarios we studied the aggregation of the naphthalenethiol-stabilized Au NPs in a DMF/water mixture by using polymer encapsulation as a means to trap intermediates (Figure 22d).[93a] The addition of salt resulted in the NPs aggregating, but the degree of aggregation, as judged by the shifting of the longitudinal plasmon absorption, stopped progressing after 12–16 h. Although more salt led to more extensive aggregation (Figure 22a,b), diluting an aggregated sample did not cause the NP chains to dissociate (Figure 22c).[93a] Clearly, the aggregates were not dynamically dissociating and reaggregating, which is inconsistent with scenario 1. Moreover, globular aggregates formed

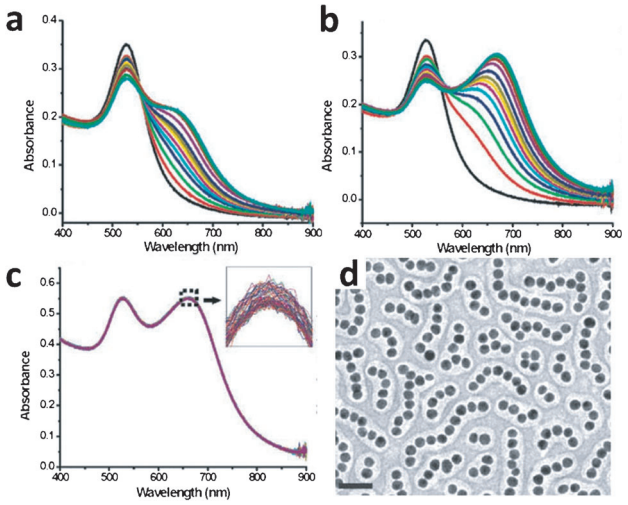

Figure 22. a,b) UV/Vis kinetics of the NP solution, where the [NaCl] was kept constant at 0.55 and 0.88 mM, respectively. The spectra were collected at $t = 0$, 1, 2, 3, 4, 5, 6, 7, 8, 10, 12, 14, and 16 h; c) UV/Vis kinetics of preaggregated Au chains after diluting the sample to reduce the [NaCl]. d) TEM image of the linear chains preserved by polymer encapsulation. Scale bar is 50 nm. Reprinted from Ref. [93a] with permission. Copyright 2010 Royal Society of Chemistry.

by rapid aggregation cannot be converted into chains. Along with other evidence, we proposed that scenario 2 should be applicable to our system.[93a] We believe that charge repulsion is the dominant factor at the transition state.[95] In other words, at the transition state, the NPs do not even touch each other and the shorter-range interactions (bonding, van der Waals, etc.) have no effect. Other key observables are also consistent with the hypothesis. With the progress of aggregation, the clusters increase in size/length, which leads to stronger cluster–cluster repulsion [Eq. (8)] and thus stopping the aggregation (Figure 22a). With more salt in the system, the aggregation can progress further before being stopped (Figure 22b). These observations cannot be explained by the interactions between a point charge and an induced dipole, which should become stronger as the cluster size increases.

6. Self-Assembly of Amphiphiles

Soft nanomaterials typically refer to those made of supra- and macromolecules.[116] Their self-assembled nanostructures, especially those made of amphiphilic block copolymers, exhibit rich morphologies such as spheres, cylinders, and vesicles, thus complementing the structural variety of inorganic nanostructures.[117] This unique feature lies in the phase-segregation of amphiphilic polymers, where the thickness of the polymer domains is limited by the physical length of the polymer chains. This leads to a different set of rules governing the spontaneous formation of cylinders and vesicles.

To understand the evolution of micelles it is critical to identify and distinguish the different types of processes therein. As a collection of polymer micelles evolve from spheres into cylinders and then vesicles, their growth in size is usually achieved by the aggregation of the micelles, which is a distinctively different process from the structural evolution of the individual micelles. Without aggregation, a spherical micelle simply does not have enough material to build a cylinder or vesicle. Overly stretching a spherical micelle would give ultrathin cylinders or vesicles, which have never been observed experimentally. The process of structural evolution can be further separated into two stages: the coalescence of the aggregated micelles and the flowing of the merged domain towards a preferred shape. As will be discussed in Section 6.3, these processes likely involve different kinds of barriers. In addition to the aggregation and structural evolution, the joining of individual polymer molecules to the micelles (micellization) is also a distinct process, which is particularly important when the critical micelle concentration (CMC) is changing during the experiment, for example, when water is added to a DMF solution.[118] Furthermore, the growth of polymer chains, if occurring, is another different process. In experiments, multiple processes are often concurrent and entangled.

To enable thermodynamic and kinetic arguments to be made, the different processes need be treated separately in the context of the overall process. The aggregation and coalescence of micelles almost never reaches the end point, that is, a single polymer particle, but the shape evolution of the individual polymer nanostructures often leads to the most stable states.

6.1. Thermodynamic Analysis

Without phase segregation, the formation of polymer NPs is almost the same as that of amorphous inorganic NPs. For example, short-chain PS is soluble in DMF, but once it becomes oversaturated (by the growth of PS chains or addition of water into the solution, etc.), the polymer will aggregate into NPs. Depending on the size of the polymer, it can be treated either as a molecule (Section 3) or a NP (Section 5). The driving force is the reduction in the PS–solvent interfacial energy, and hence the minimization of the S/V ratio leads to the formation of spherical NPs (Section 2.2). The size of such NPs is only limited by the aggregation kinetics, not by the polymer behavior (Figure 23a). For a collection of NPs, reducing the number of particles and increasing their sizes is always thermodynamically favorable, as it leads to a lower surface energy of the whole system.

The situation for shape determination is actually very similar for a more complex system where molecules and polymers strongly interact with each other. As long as there is no crystallinity and phase segregation, the mixture of molecules behave the same as a single homogeneous phase, for example, supramolecules with extensive host–guest interactions or polymers decorated with supramolecules.[119] When such mixtures are rendered insoluble in solution, the products are typically spherical.

In contrast, the situation is drastically different for an amphiphilic copolymer, for example, PS-*b*-PAA, in water (Figure 23b). The soluble PAA block and insoluble PS block cause the polymer to self-assemble into micelles, with the PS

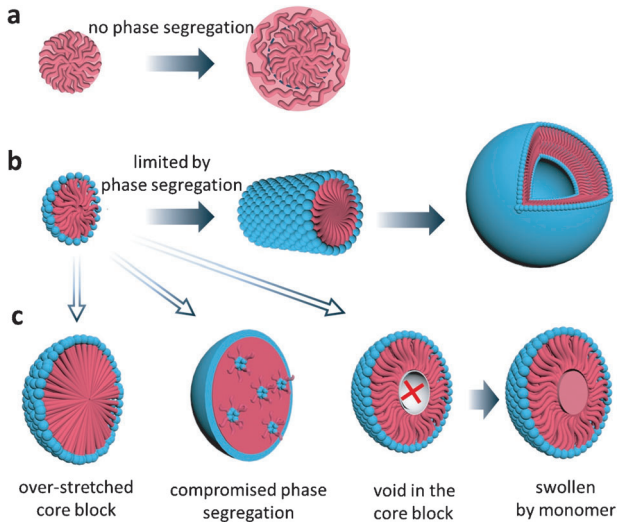

Figure 23. Thermodynamically favorable morphologies of a) homopolymer; b) amphiphilic copolymers with increasing domain size while maintaining phase segregation; c) the possible scenarios when forming massive aggregates. The hydrophilic section is represented in blue and the hydrophobic section in red.

blocks squeezed in the core and the PAA blocks dissolved in the solution, thereby forming a corona.[117a,120] Such a phase-segregated configuration is stable because it maximizes the favorable interactions among the polymer chains and between the polymer and the solvent. Importantly, the thickness of the PS domain is limited by the length of the PS chains, and stretched chains are entropically unfavorable.[72,121] In other words, a PS chain has numerous conformations, among which the straightened conformations are highly improbable and thus encounter an entropic penalty. As summarized in Figure 23c, forming massive polymer aggregates would demand 1) over-stretched PS blocks, 2) a void in the PS domain, or 3) embedding of the PAA blocks in the PS domain (partially compromised phase segregation). These options are energetically unfavorable, but can be induced under specific conditions, such as the swelling caused by the addition of homo-PS,[72] the protonation of the PAA blocks,[96c] etc.[122]

There are two main competing factors that determine the size and shape of the micelles under the restriction of phase segregation.[96a] On one hand, increasing the size of the PS domain would reduce the PS–solvent interfacial energy per unit volume (Section 2.2). Hence, the solvophobic interactions are part of the driving force. It is important to note that, for a given amount of PS, reducing the PS–solvent interface necessitates an increase in the interactions within the PS domain (van der Waals interactions, etc.), which is also part of the driving force. On the other hand, the steric and charge repulsion between the crowded PAA blocks on the micelle surface would resist the over-growth of the micelle.

Hence, the size and morphology of polymer nanostructures are determined by three interacting factors: the stretching of the PS block limits the thickness of the hydrophobic domain; the reduction in the interfacial energy favors larger micelles; and the repulsion between the PAA blocks

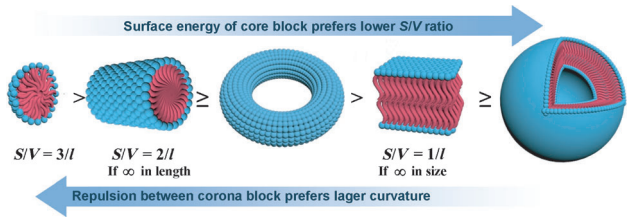

Figure 24. The choice of shapes under the influence of two competing trends, in the sequence of a sphere, a cylinder (the caps are not shown), a circular ring, a lamella (the edges are not shown), and an enclosed vesicle.

favors higher curvature and thus smaller micelles (Figure 24). Elongating a micelle into a cylinder would allow it to grow, thereby reducing the surface energy (the S/V ratio) without compromising the phase segregation. A further step in this direction is to extend the cylinder into a lamella or vesicle.

The popular theory explaining the shape of micelles invokes the "packing parameter" p, which is a geometric indicator describing the hydrophobic section of an average polymer molecule in the micelle [Eq. (10)].

$$p = V/al \tag{10}$$

Here, V is the volume of the hydrophobic section, l is the length of the hydrophobic chain normal to the interface (i.e. half of the thickness of the hydrophobic domain), and a is the contact area between the hydrophobic section and the hydrophilic head.[47b,117a,123] Although the size and shape of an average polymer molecule are unknown and these variables are not quantifiable, the packing parameter can be used to explain the major trends in the shape evolution as follows. Spherical micelles are preferred when the repulsion between the PAA blocks is the dominant factor (that is, an average molecule has a large hydrophilic section). Assuming that the hydrophobic section of an average molecule is a cone with a as the base area and l as the height, one can conclude that $p \leq 1/3$. Cylindrical micelles are the most stable state when the repulsion is weaker. The parameter can be assigned, on the basis of an average sector in the cylinder, as $1/3 \leq p \leq 1/2$. When the repulsion is a minor factor and lamellar or vesicular micelles are favored, one can deduce from an average segment in the layer that $1/2 \leq p \leq 1$. As such, the packing parameter is determined from the observed shapes, rather than a quantifiable indicator that predicates the shapes.

Although the argument of the packing parameter focuses on the shape of an average molecule, the S/V ratio of the overall micelle has a physical meaning. Basically, the ratio gives a measure of the surface area per unit amount of material, thus reflecting the relative strength of the surface energy. Hence, a small ratio is energetically preferred. If the small variation[121b] in the thickness of the hydrophobic domain (defined as $2l$) is not considered, the S/V ratio decreases in the following order: sphere $(3/l)$ > cylinder $(2/l)$ > vesicle $(1/l$; Figure 24). Comparing these values under the boundary conditions, it is clear that this argument is equivalent to that of the packing parameter, although it is presented in a different form.

In thermodynamic arguments, the minimum energy structure should ideally be predicted on the basis of the free energy terms. We can use the packing parameter or the S/V ratio as the geometric indicators of the general trends, but unless they are linked to the energy terms they do not help the understanding. In the above discussion, we tried to link the S/V ratio to the dominant surface energy term, the stretching of the PS blocks to the dominant entropy term, in addition to the repulsion potential of the PAA blocks. Thus, the general trends can be deduced on the basis of energy arguments. Another advantage of the S/V ratio is that it can be readily quantified from the experimentally observed structures, not only for the spheres, cylinders, and vesicles, but also for the trapped intermediates between their transitions (Section 6.2).

With these basic principles, the common thermodynamic factors affecting the shape of micelles can be understood.[117a,120] Longer PAA blocks or blocks with higher charge densities (higher degree of deprotonation) would lead to stronger repulsion, thus driving the transformation in Figure 24 to the left. Neutralizing the surface charge[96a,124] or shielding the charge repulsion (by adding a salt[96b] or an additive of opposite charge, such as polyamine molecules)[125] drives the transformation to the right. Using a PS-*b*-PAA with longer PS blocks would lead to less surface density on the PAA blocks, thus favoring the right side.[126] Increasing the PS–solvent interfacial energy (using more solvophobic polymer blocks than PS, using a more polar solvent mixture, etc.) leads to a larger driving force for reducing the S/V ratio, thus favoring the right side, whereas decreasing the interfacial energy (swelling the polymer domain using more solvophilic additives, etc.) favors the left side. Stronger cohesive interactions in the hydrophobic domain[123b] (better packing, additional bonding interactions, etc.) means that the reduction in the S/V ratio would bring about a larger driving force (Section 2.2), thus favoring the right side.

The stretching of the PS blocks in the hydrophobic domain can also be tuned to affect the polymer morphology. For example, homo-PS can be used as the filler or swelling agent, so that it can accumulate at the center of the hydrophobic domain (Figure 23c), thereby reducing the stretching of the PS blocks in the PS-*b*-PAA, and thus favoring the structures with higher curvature (the left side in Figure 24).[72] In other words, the filler allows the micelles to grow in size without compromising the phase segregation, so there is less driving force for them to change to a different shape.

For other types of amphiphilic polymers, such as non-ionic diblock copolymers,[127] triblock copolymers,[128] graft copolymers,[129] or dendritic polymers,[130] the nature and strength of the interactions are different but the basic principles are similar. The same is true for small-molecule surfactants such as sodium dodecylsulfate (SDS) and CTAB. Of course, the arguments here are based on complete phase segregation. Without phase separation, the formation of massive aggregates would be more favorable.

Blending different polymers or starting from different micellar states (compare to Section 6.2.2) should not affect the final product when it is under thermodynamic control. At full equilibration, the system should always rest at the most stable state. Eisenberg and co-workers showed that a mixture of PS-*b*-PAA with PAA of different lengths (increased polydispersity) gave smaller vesicles, where the short PAA chains were segregated in the inner concave surface as a result of their weaker repulsion.[131]

As is typical for thermodynamic analysis, the above discussion compares the relative stability of the end states of micellar morphologies. That is, the polymer nanostructures are presumed to have fully equilibrated and the transformation pathways between the states are irrelevant. However, having a driving force towards a certain shape does not necessarily mean that the shape can be reached, and the structures observed in the experiments are not necessarily fully equilibrated. Kinetic analysis is of critical importance to study these issues.

6.2. Kinetic Analysis

The key to discussing kinetics is to identify the main barriers and relate them to the detailed shape evolution of the micelles. Given the many concurrent processes, treating the overall process as a "black box" for data analysis can easily cause confusion. The discussion must address the specific nature of each process. For convenience of discussion, here we use the amphiphilic diblock copolymer PS-*b*-PAA as an example.

First, let's consider the aggregation of two micelles, which is a fundamental step in the overall process. Usually the barrier preventing their effective collision is the steric and/or charge repulsion between the coronal blocks. After making contact, the subsequent merging of the polymer domains establishes strong "bonding" interactions, thereby deterring their dissociation. At a molecular level, the reorganization of the polymer blocks is a process that cannot be ignored. Specifically, the hydrophilic blocks (PAA) need to move away from the contact point for the hydrophobic domains to merge. However, before making contact, "preparing" the micelles in such a way would be statistically improbable. Upon aggregation, it is likely that some PAA chains will be embedded in the partially merged PS domain at the contact point, when the high density of the PAA blocks on the micelle surface is considered.[47b] This creates an additional barrier that is often overlooked. It may slow down or even prevent the merging of micelles (Section 6.2.1).

The initial encounters of a collection of micelles through random collision (before the merging of polymer domains) should be similar to the aggregation of inorganic NPs (Section 5.2).[91,92b] However, in contrast to the case of inorganic NPs, there is usually extensive coalescence of the aggregated polymer domains, which makes the aggregation process irreversible. With the simultaneous progress of the aggregation and structural evolution, the outcome depends on the relative rate of the two. There are a few possible scenarios: 1) When the structural evolution is extremely efficient, it will be hard to trap the micelles at the intermediate shapes. With most of the micelles adopting the preferred morphology, the outcome is usually nice and clean. 2) When the structural evolution is extremely slow, most of

the products will be intermediates. Such messy results can be easily overlooked. 3) For the intermediate cases, timing is critical. The probability of collision should be second-order in the concentration of the micelles, which diminishes with the progress of aggregation. The average volume of micelles typically increases by more than 10 times, thereby leading to $< 1/10$ of the initial micelle concentration and $< 1/100$ of the initial collision rate.

After merging, the polymer domain still needs to transform and somehow find the most stable structure. Clearly, the polymer does not "know" the direction and the overall process is guided by the "invisible hands" of the thermodynamics, just like the equilibration of a liquid droplet towards a spherical shape (Section 3.2.1). Although the thermodynamics are well-established, as discussed above, the pathways of transformation remain elusive. What are the intermediate states and what are the barriers? For example, it is difficult to conceive the detailed steps of how a cylinder would evolve into an enclosed vesicle. Indeed, the conversion from a lamellar sheet to an enclosed vesicle is nontrivial, with multiple steps of folding, stitching, and removal of the overlapped regions. Unfortunately, topics such as these have been rarely discussed in the literature.[89a,c,124,132]

6.2.1. *Kinetic Pathway in the Transformation from Cylinder to Vesicle*

Several bowl-like structures have been reported as intermediates during the cylinder-to-vesicle transformation.[121a,132a,g] In our laboratory, we focused on PS_{154}-*b*-PAA_{49} micelles, which evolve slowly (in hours) because of their long PAA blocks. The conditions were selected such that the vesicles are the thermodynamic end point and the polymer micelles are made to slowly evolve towards it. This allowed us to trap a series of intermediates under the same conditions and led to a complete pathway being proposed (Figure 25). A cylindrical micelle first flattens to give a lamellar section, which depresses to give a bowl-like intermediate. The continuous "flow" of polymer from the tethered cylinder provides the material necessary for the transformation. As the bowl deepens, it passes the stage of half-vesicle and then the opening tightens. A vesicle is eventually generated with the closing of the opening and the detachment of the tethered cylinder. It is important to note that most of these steps are achieved by the simple "flowing" of the polymer domains.

Calculation of the S/V ratio for the intermediates showed no apparent energy barrier in the shape evolution (Figure 26 f). The pathway is monotonously downhill in terms of the decreasing S/V ratio. This result is counterintuitive because should there be no energy barrier, all structures with sufficient materials would have evolved to vesicles, in direct conflict with the experimental observations. To explain the kinetically trapped intermediates, we propose that the main energy barrier originates from the molecular reorganization within the micelles.

Simple geometric analysis of the micelles can illustrate the importance of the molecular reorganization therein. Even bending a bilayer membrane would induce compressive stain

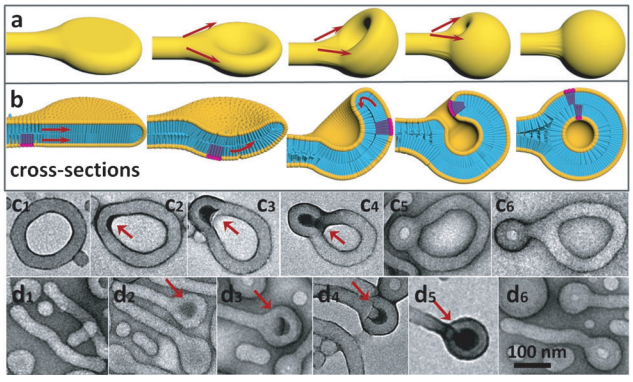

Figure 25. a) Progress in structural transformation from a cylinder to vesicle. b) A cross-sectional view of the process, where a section is highlighted in purple to show the flow of the polymer domain. c,d) Selected TEM images showing the typical intermediates during the cylinder-to-vesicle transformation. Reprinted from Ref. [47a] with permission. Copyright 2013 Wiley-VCH.

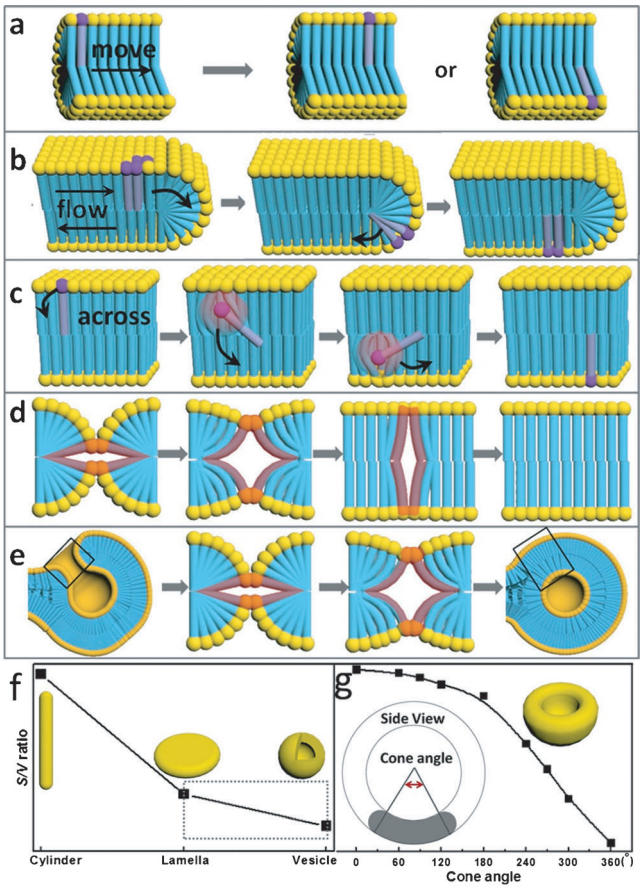

Figure 26. Analysis of kinetic barriers from the point of view of molecular reorganization: a) parallel movement of amphiphiles within a micelle; b) "flowing" of an entire domain back and forth; c) movement of amphiphiles directly across a hydrophobic domain; d) merging of micellar fronts (the reverse process is the severing of the micelle); e) elimination of the pinhole at the final stage of vesicle formation. f) Calculated S/V ratio of a cylinder, lamella, and vesicle. g) Calculated S/V ratio for the bowl-like intermediates during the lamella to vesicle transition. Reprinted from Ref. [47a] with permission. Copyright 2013 Wiley-VCH.

in the inner layer and tensile strain in the outer layer. To relieve the strains and achieve permanent bending, molecules must move from the inner to the outer layer, thereby creating an extra step which must be considered.

The relative easiness of the molecular reorganization can be evaluated by analyzing the strength of the molecular interactions. More specifically, the hydrophobic blocks are stabilized by strong interactions (van der Waals, hydrophobic interactions, etc.) and so are the hydrophilic blocks (solvation, entropy, hydrogen bonding, etc.), but there are only weak interactions between the nonpolar hydrophobic and polar hydrophilic blocks. Thus, moving a molecule parallel within a domain (Figure 26a) or a flowing of the domain (Figure 26b) would encounter small energy barriers because few interactions are broken. On the other hand, the movement of a molecule across a membrane (Figure 26c), the merging and severing of micelles (Figure 26d), and the closing of partial vesicles (Figure 26e) would encounter a large energy barrier as a result of the compromised molecular interactions. The red regions in Figure 26c–e illstrate the possible unfavorable interactions. The fact that they cannot be avoided in the transformation process suggests the presence of high-energy intermediates. However, it should be noted that creating voids in the PS domain (Figure 26d,e) is only one possibility; it is by no means the only pathway.

In the above discussion, we seek to go beyond the shape analysis of the intermediates and try to establish the kinetic pathway through energy-based arguments. The experimental observations in our studies and in the literature were found to be consistent with the mechanistic proposal. Lower energy barriers are expected in the polymer transformation if shorter or less charged hydrophilic blocks are used,[47b,96b,125,133] or if the hydrophobic blocks have weaker interactions with each other (so that they can easily flow across each other). The relative ease of the polymer transformation can be evaluated on the basis of the time, temperature, swelling conditions, etc.[47a]

6.2.2. *Kinetic Control in Complex Systems*

A higher level of structural complexity can be achieved with amphiphilic polymers through kinetic control. For example, mixing different amphiphilic polymers was found to give discoid morphologies such as triangles and squares.[134] These polymers have different packing parameters and presumably also different mobilities. The segregation of the polymers led to hemispherical caps that partially locked the structure during its shape transformation, eventually leading to micelles with multiple geometries.

On the other hand, monovalent and divalent colloidal building blocks made of amphiphilic block copolymers have been used to create hierarchical structures.[135] These building blocks were essentially phase-segregated micelles, where the hydrophobic domains were kinetically locked during the subsequent assembly. As such, the valency of the building blocks could exert its effects in the assembly process, thereby giving binary and ternary aggregates.

It is conceivable that the final product under kinetic control would be highly dependent on the starting state and the exact pathways. Resolving the pathway would clearly be more challenging with multiply interacting polymers.

6.3. The T-K Problem

Considering the structural complexity of amphiphilic polymers and the multiple processes involved in their shape transformation, it is a challenge to determine if an observed structure is thermodynamically or kinetically controlled.

In polymer systems, the experimental parameters can often affect both the thermodynamic driving force and the kinetic barrier. This is more likely than in other systems. Thus, designing the experimental condition is critical for reducing the ambiguity. Adding water to the DMF/water solution causes the PS-*b*-PAA micelles to transform towards vesicles (the right side in Figure 24), but it also causes the deswelling of the polymer domains, thus making them evolve slower.[47b,136] The addition of acid[124] or polyamine[125] can neutralize the negative charge of the PAA blocks, thereby reducing charge repulsion. As a consequence, the micelles would evolve towards vesicles (thermodynamics), but it also facilitates molecular reorganization (kinetics). Increasing the length of the hydrophobic blocks by polymerization would alter both the thermodynamic end state and the mobility of the polymer domain.[124]

Thermodynamic arguments have often been invoked to explain the formation of polymer nanostructures, in particular vesicles. However, the shape in itself is not sufficient evidence. For example, the addition of acid can cause PSPAA micelles to evolve to vesicles, but reversing the condition (by neutralization with base) normally does not convert the vesicles back into spherical micelles, likely because of the large energy barrier for severing the polymer domains (the reverse process of Figure 25d). As such, the vesicles would be thermodynamically unstable but kinetically trapped. In contrast, we can conceive a hypothetic scenario where the aggregation process is very slow but the structural evolution is efficient. Thus, all the nanostructures would evolve to the minimum energy shapes. If the process can be trapped at an early stage when many of the nanostructures do not have sufficient materials to form vesicles, such a condition would be very interesting. The "intermediates" would be thermodynamically stable with the given amount of materials, but they are not stable if allowed to grow by aggregation. In this special case, observing a bowl-like intermediate does not necessarily mean that it is kinetically controlled (in terms of its structural evolution).

7. Summary and Outlook

The microscopic processes in the formation of nanostructures are random and dynamic. Among the chaos, orderly nanostructures are known to emerge, including regular shapes, uniform sizes, and extensive superstructures. Such ordering is the basis of nanoscience and nanotechnology, and understanding its origin is of pivotal importance. We must start from the fundamental principles of growing and assem-

bling the basic building blocks, before sophisticated nanostructures can be made for advanced applications. Establishing the mechanistic proposals on the basis of energy terms is a first step towards a rational design and systems approach.

By using simple geometric analysis and logical deduction we demonstrated that it is indeed possible to compare the relative stabilities of nanostructures during their growth, assembly, and shape evolution. The detailed processes therein were described and carefully analyzed, so that the mechanistic proposals were unambiguously presented. The key theories and hypotheses in the literature have been incorporated in our discussion. By using specific examples we illustrated how the various factors interacted with each other, and how these interactions led to the observables. We highlighted the fundamental differences between the thermodynamically and kinetically controlled scenarios and advocated such a distinction be used in mechanistic proposals.

The principles of thermodynamics and kinetics are universal. Applying these arguments in nanosynthesis is necessary and urgent. The fact that the system is imperfect at the moment is not a reason to avoid it, simply a reason for more researchers to improve it.

*We thank the A*Star (SERC 112-120-2011) of Singapore and Singapore National Research Foundation (NRF) (Sustainable Energy (SinBeRISE) CREATE Programme through the Singapore-Berkeley Research Initiative) for financial support.*

Received: March 4, 2014
Published online: December 23, 2014

[1] a) F. Baletto, R. Ferrando, *Rev. Mod. Phys.* **2005**, *77*, 371 – 423; b) J. E. McMurry, *Organic Chemistry*, 7th ed., Brooks/Cole, Belmont, CA, **2008**.
[2] a) A. G. Catchpole, E. D. Hughes, C. K. Ingold, *J. Chem. Soc.* **1948**, 8 – 17; b) H. O. House, B. A. Tefertiller, H. D. Olmstead, *J. Org. Chem.* **1968**, *33*, 935 – 942; c) J. d'Angelo, *Tetrahedron* **1976**, *32*, 2979 – 2990.
[3] A. Cooksy, Physical Chemistry: Thermodynamics, Statistical Mechanics & Kinetics, Pearson, Boston: **2014**.
[4] P. Zhang, F. Xu, A. Navrotsky, J. S. Lee, S. Kim, J. Liu, *Chem. Mater.* **2007**, *19*, 5687 – 5693.
[5] a) Y. N. Xia, G. M. Whitesides, *Annu. Rev. Mater. Sci.* **1998**, *28*, 153 – 184; b) J. C. Hulteen, D. A. Treichel, M. T. Smith, M. L. Duval, T. R. Jensen, R. P. Van Duyne, *J. Phys. Chem. B* **1999**, *103*, 3854 – 3863; c) B. D. Gates, Q. Xu, M. Stewart, D. Ryan, C. G. Willson, G. M. Whitesides, *Chem. Rev.* **2005**, *105*, 1171 – 1196.
[6] M. A. Fox, J. K. Whitesell, *Organic Chemistry*, Jones and Bartlett, Sudbury, **1997**.
[7] a) A. S. Barnard, *J. Mater. Chem.* **2006**, *16*, 813 – 815; b) A. S. Barnard, *Acc. Chem. Res.* **2012**, *45*, 1688 – 1697.
[8] C. Shang, Z.-P. Liu, *J. Chem. Theory Comput.* **2013**, *9*, 1838 – 1845.
[9] a) D. Chandler, *Nature* **2005**, *437*, 640 – 647; b) W. Blokzijl, J. B. F. N. Engberts, *Angew. Chem.* **1993**, *105*, 1610 – 1650; *Angew. Chem. Int. Ed. Engl.* **1993**, *32*, 1545 – 1579; c) K. J. M. Bishop, C. E. Wilmer, S. Soh, B. A. Grzybowski, *Small* **2009**, *5*, 1600 – 1630.
[10] T. P. Silverstein, *J. Chem. Educ.* **1998**, *75*, 116.
[11] N. T. Southall, K. A. Dill, A. D. J. Haymet, *J. Phys. Chem. B* **2002**, *106*, 521 – 533.
[12] a) C. N. R. Rao, G. U. Kulkarni, P. J. Thomas, P. P. Edwards, *Chem. Eur. J.* **2002**, *8*, 28 – 35; b) I. A. Mudunkotuwa, V. H. Grassian, *J. Environ. Monit.* **2011**, *13*, 1135 – 1144; c) R. Dingreville, J. M. Qu, M. Cherkaoui, *J. Mech. Phys. Solids* **2005**, *53*, 1827 – 1854; d) G. Ouyang, C. X. Wang, G. W. Yang, *Chem. Rev.* **2009**, *109*, 4221 – 4247.
[13] a) R. C. Cammarata, K. Sieradzki, *Annu. Rev. Mater. Sci.* **1994**, *24*, 215 – 234; b) K. L. Johnson, K. Kendall, A. D. Roberts, *Proc. R. Soc. London Ser. A* **1971**, *324*, 301 – 313.
[14] J. C. Love, L. A. Estroff, J. K. Kriebel, R. G. Nuzzo, G. M. Whitesides, *Chem. Rev.* **2005**, *105*, 1103 – 1170.
[15] N. Pradhan, D. Reifsnyder, R. Xie, J. Aldana, X. Peng, *J. Am. Chem. Soc.* **2007**, *129*, 9500 – 9509.
[16] J. B. Schlenoff, M. Li, H. Ly, *J. Am. Chem. Soc.* **1995**, *117*, 12528 – 12536.
[17] a) Y. Feng, Y. Wang, H. Wang, T. Chen, Y. Y. Tay, L. Yao, Q. Yan, S. Li, H. Chen, *Small* **2012**, *8*, 246 – 251; b) G. Lu, S. Z. Li, Z. Guo, O. K. Farha, B. G. Hauser, X. Y. Qi, Y. Wang, X. Wang, S. Y. Han, X. G. Liu, J. S. DuChene, H. Zhang, Q. C. Zhang, X. D. Chen, J. Ma, S. C. J. Loo, W. D. Wei, Y. H. Yang, J. T. Hupp, F. W. Huo, *Nat. Chem.* **2012**, *4*, 310 – 316; c) M. Sindoro, Y. Feng, S. Xing, H. Li, J. Xu, H. Hu, C. Liu, Y. Wang, H. Zhang, Z. Shen, H. Chen, *Angew. Chem.* **2011**, *123*, 10072 – 10076; *Angew. Chem. Int. Ed.* **2011**, *50*, 9898 – 9902; d) H. Li, H. L. Xin, D. A. Muller, L. A. Estroff, *Science* **2009**, *326*, 1244 – 1247.
[18] Y. Yin, A. P. Alivisatos, *Nature* **2005**, *437*, 664 – 670.
[19] a) S. Polarz, *Adv. Funct. Mater.* **2011**, *21*, 3214 – 3230; b) C. Herring, *Phys. Rev.* **1951**, *82*, 87 – 93.
[20] a) Z. L. Wang, *J. Phys. Chem. B* **2000**, *104*, 1153 – 1175; b) L. Vitos, A. V. Ruban, H. L. Skriver, J. Kollar, *Surf. Sci.* **1998**, *411*, 186 – 202.
[21] a) C.-Y. Chiu, Y. Li, L. Ruan, X. Ye, C. B. Murray, Y. Huang, *Nat. Chem.* **2011**, *3*, 393 – 399; b) W. A. Al-Saidi, H. Feng, K. A. Fichthorn, *Nano Lett.* **2012**, *12*, 997 – 1001; c) B. Wu, N. Zheng, *Nano Today* **2013**, *8*, 168 – 197; d) Q. Chen, N. V. Richardson, *Prog. Surf. Sci.* **2003**, *73*, 59 – 77; e) Y. N. Xia, Y. J. Xiong, B. Lim, S. E. Skrabalak, *Angew. Chem.* **2009**, *121*, 62 – 108; *Angew. Chem. Int. Ed.* **2009**, *48*, 60 – 103; f) C. R. Bealing, W. J. Baumgardner, J. J. Choi, T. Hanrath, R. G. Hennig, *ACS Nano* **2012**, *6*, 2118 – 2127; g) J. J. De Yoreo, P. M. Dove, *Science* **2004**, *306*, 1301 – 1302.
[22] M. Liu, Y. Zheng, L. Zhang, L. Guo, Y. Xia, *J. Am. Chem. Soc.* **2013**, *135*, 11752 – 11755.
[23] a) R. D. James, K. F. Hane, *Acta Mater.* **2000**, *48*, 197 – 222; b) A. G. Evans, R. M. Cannon, *Acta Metall.* **1986**, *34*, 761 – 800.
[24] a) P. W. Voorhees, *J. Stat. Phys.* **1985**, *38*, 231 – 252; b) P. W. Voorhees, *Annu. Rev. Mater. Sci.* **1992**, *22*, 197 – 215.
[25] a) Q. Zhang, W. Li, L.-P. Wen, J. Chen, Y. Xia, *Chem. Eur. J.* **2010**, *16*, 10234 – 10239; b) D. Seo, J. C. Park, H. Song, *J. Am. Chem. Soc.* **2006**, *128*, 14863 – 14870; c) C.-H. Kuo, T.-F. Chiang, L.-J. Chen, M. H. Huang, *Langmuir* **2004**, *20*, 7820 – 7824.
[26] a) V. K. LaMer, R. H. Dinegar, *J. Am. Chem. Soc.* **1950**, *72*, 4847 – 4854; b) J. Park, J. Joo, S. G. Kwon, Y. Jang, T. Hyeon, *Angew. Chem.* **2007**, *119*, 4714 – 4745; *Angew. Chem. Int. Ed.* **2007**, *46*, 4630 – 4660.
[27] D. Kaščiev, *Nucleation: Basic Theory with Applications*, Butterworth Heinemann, Oxford, **2000**.
[28] T. Wang, D. LaMontagne, J. Lynch, J. Q. Zhuang, Y. C. Cao, *Chem. Soc. Rev.* **2013**, *42*, 2804 – 2823.
[29] J. R. Fried, *Polymer Science & Technology*, 2nd ed., Prentice Hall, Upper Saddle River, NJ, **2013**.
[30] a) M. Brust, M. Walker, D. Bethell, D. J. Schiffrin, R. Whyman, *J. Chem. Soc. Chem. Commun.* **1994**, 801 – 802; b) N. R. Jana, L. Gearheart, C. J. Murphy, *Langmuir* **2001**, *17*, 6782 – 6786; c) M. Brust, J. Fink, D. Bethell, D. J. Schiffrin, C. Kiely, *J. Chem. Soc. Chem. Commun.* **1995**, 1655 – 1656.

[31] a) X. Peng, L. Manna, W. Yang, J. Wickham, E. Scher, A. Kadavanich, A. P. Alivisatos, *Nature* **2000**, *404*, 59 – 61; b) C. B. Murray, D. J. Norris, M. G. Bawendi, *J. Am. Chem. Soc.* **1993**, *115*, 8706 – 8715; c) T. Hyeon, *Chem. Commun.* **2003**, 927 – 934.

[32] a) S. G. Kwon, T. Hyeon, *Small* **2011**, *7*, 2685 – 2702; b) C. de Mello Donegá, P. Liljeroth, D. Vanmaekelbergh, *Small* **2005**, *1*, 1152 – 1162; c) C. B. Murray, C. R. Kagan, M. G. Bawendi, *Annu. Rev. Mater. Sci.* **2000**, *30*, 545 – 610.

[33] H. Sun, J. He, J. Wang, S.-Y. Zhang, C. Liu, T. Sritharan, S. Mhaisalkar, M.-Y. Han, D. Wang, H. Chen, *J. Am. Chem. Soc.* **2013**, *135*, 9099 – 9110.

[34] A. R. Tao, S. Habas, P. Yang, *Small* **2008**, *4*, 310 – 325.

[35] Y. Sun, Y. Xia, *Science* **2002**, *298*, 2176 – 2179.

[36] a) J. Zeng, Y. Zheng, M. Rycenga, J. Tao, Z.-Y. Li, Q. Zhang, Y. Zhu, Y. Xia, *J. Am. Chem. Soc.* **2010**, *132*, 8552 – 8553; b) Y. Wang, D. Wan, S. Xie, X. Xia, C. Z. Huang, Y. Xia, *ACS Nano* **2013**, *7*, 4586 – 4594.

[37] Y. Ma, Q. Kuang, Z. Jiang, Z. Xie, R. Huang, L. Zheng, *Angew. Chem.* **2008**, *120*, 9033 – 9036; *Angew. Chem. Int. Ed.* **2008**, *47*, 8901 – 8904.

[38] a) M. L. Personick, C. A. Mirkin, *J. Am. Chem. Soc.* **2013**, *135*, 18238 – 18247; b) M. R. Langille, M. L. Personick, J. Zhang, C. A. Mirkin, *J. Am. Chem. Soc.* **2012**, *134*, 14542 – 14554.

[39] a) N. Wang, Y. Cai, R. Q. Zhang, *Mater. Sci. Eng. R* **2008**, *60*, 1 – 51; b) M. Grzelczak, J. Perez-Juste, P. Mulvaney, L. M. Liz-Marzan, *Chem. Soc. Rev.* **2008**, *37*, 1783 – 1791; c) Y. N. Xia, P. D. Yang, Y. G. Sun, Y. Y. Wu, B. Mayers, B. Gates, Y. D. Yin, F. Kim, Y. Q. Yan, *Adv. Mater.* **2003**, *15*, 353 – 389.

[40] V. Germain, J. Li, D. Ingert, Z. L. Wang, M. P. Pileni, *J. Phys. Chem. B* **2003**, *107*, 8717 – 8720.

[41] a) Y. Xiong, J. M. McLellan, J. Chen, Y. Yin, Z.-Y. Li, Y. Xia, *J. Am. Chem. Soc.* **2005**, *127*, 17118 – 17127; b) Y. Xiong, I. Washio, J. Chen, H. Cai, Z.-Y. Li, Y. Xia, *Langmuir* **2006**, *22*, 8563 – 8570; c) J. Goebl, Q. Zhang, L. He, Y. Yin, *Angew. Chem.* **2012**, *124*, 567 – 570; *Angew. Chem. Int. Ed.* **2012**, *51*, 552 – 555.

[42] Y. Sun, B. Mayers, T. Herricks, Y. Xia, *Nano Lett.* **2003**, *3*, 955 – 960.

[43] C. Lofton, W. Sigmund, *Adv. Funct. Mater.* **2005**, *15*, 1197 – 1208.

[44] a) M. J. Bierman, Y. K. A. Lau, A. V. Kvit, A. L. Schmitt, S. Jin, *Science* **2008**, *320*, 1060 – 1063; b) S. A. Morin, M. J. Bierman, J. Tong, S. Jin, *Science* **2010**, *328*, 476 – 480.

[45] a) J. Gao, C. M. Bender, C. J. Murphy, *Langmuir* **2003**, *19*, 9065 – 9070; b) C. J. Johnson, E. Dujardin, S. A. Davis, C. J. Murphy, S. Mann, *J. Mater. Chem.* **2002**, *12*, 1765 – 1770.

[46] X. Huang, S. Tang, X. Mu, Y. Dai, G. Chen, Z. Zhou, F. Ruan, Z. Yang, N. Zheng, *Nat. Nanotechnol.* **2011**, *6*, 28 – 32.

[47] a) C. Liu, L. Yao, H. Wang, Z. R. Phua, X. Song, H. Chen, *Small* **2014**, *10*, 1332 – 1340; b) C. Liu, G. Chen, H. Sun, J. Xu, Y. Feng, Z. Zhang, T. Wu, H. Chen, *Small* **2011**, *7*, 2721 – 2726.

[48] C. J. Murphy, N. R. Jana, *Adv. Mater.* **2002**, *14*, 80 – 82.

[49] a) N. R. Jana, L. Gearheart, C. J. Murphy, *J. Phys. Chem. B* **2001**, *105*, 4065 – 4067; b) B. Nikoobakht, M. A. El-Sayed, *Chem. Mater.* **2003**, *15*, 1957 – 1962; c) S.-S. Chang, C.-W. Shih, C.-D. Chen, W.-C. Lai, C. R. C. Wang, *Langmuir* **1999**, *15*, 701 – 709.

[50] Z. Huo, C.-k. Tsung, W. Huang, X. Zhang, P. Yang, *Nano Lett.* **2008**, *8*, 2041 – 2044.

[51] N. Poudyal, G. S. Chaubey, V. Nandwana, C. B. Rong, K. Yano, J. P. Liu, *Nanotechnology* **2008**, *19*.

[52] a) T. J. Trentler, K. M. Hickman, S. C. Goel, A. M. Viano, P. C. Gibbons, W. E. Buhro, *Science* **1995**, *270*, 1791 – 1794; b) M. H. Huang, S. Mao, H. Feick, H. Q. Yan, Y. Y. Wu, H. Kind, E. Weber, R. Russo, P. D. Yang, *Science* **2001**, *292*, 1897 – 1899; c) M. Law, J. Goldberger, P. D. Yang, *Annu. Rev. Mater. Res.* **2004**, *34*, 83 – 122; d) W. Lu, C. M. Lieber, *J. Phys. D* **2006**, *39*, R387 – R406; e) S. Kuchibhatla, A. S. Karakoti, D. Bera, S. Seal, *Prog. Mater. Sci.* **2007**, *52*, 699 – 913; f) H. J. Fan, P. Werner, M. Zacharias, *Small* **2006**, *2*, 700 – 717.

[53] J. He, Y. Wang, Y. Feng, X. Qi, Z. Zeng, Q. Liu, W. S. Teo, C. L. Gan, H. Zhang, H. Chen, *ACS Nano* **2013**, *7*, 2733 – 2740.

[54] a) S. Iijima, T. Ichihashi, *Phys. Rev. Lett.* **1986**, *56*, 616 – 619; b) D. J. Smith, A. K. Petford-Long, L. R. Wallenberg, J. O. Bovin, *Science* **1986**, *233*, 872 – 875.

[55] a) L. Ruan, C.-Y. Chiu, Y. Li, Y. Huang, *Nano Lett.* **2011**, *11*, 3040 – 3046; b) B. J. Wiley, Y. Xiong, Z.-Y. Li, Y. Yin, Y. Xia, *Nano Lett.* **2006**, *6*, 765 – 768.

[56] a) E. Ringe, R. P. Van Duyne, L. D. Marks, *J. Phys. Chem. C* **2013**, *117*, 15859 – 15870; b) L. D. Marks, *J. Cryst. Growth* **1983**, *61*, 556 – 566.

[57] B. Wiley, T. Herricks, Y. Sun, Y. Xia, *Nano Lett.* **2004**, *4*, 1733 – 1739.

[58] A. S. Barnard, *J. Phys. Chem. B* **2006**, *110*, 24498 – 24504.

[59] a) Q. Su, D. Xie, J. Zhang, G. Du, B. Xu, *ACS Nano* **2013**, *7*, 9115 – 9121; b) A. Yasuda, N. Kawase, W. Mizutani, *J. Phys. Chem. B* **2002**, *106*, 13294 – 13298; c) L. J. Chen, W. W. Wu, *Mater. Sci. Eng. R* **2010**, *70*, 303 – 319; d) R. Sharma, *J. Mater. Res.* **2005**, *20*, 1695 – 1707; e) A. H. Zewail, *Science* **2010**, *328*, 187 – 193; f) R. Sharma, *Microsc. Res. Tech.* **2009**, *72*, 144 – 152; g) D. Li, M. H. Nielsen, J. J. De Yoreo, *Methods in Enzymology*, *Vol. 532* (Ed.: J. D. Y. James), Academic Press, **2013**, pp. 147 – 164.

[60] a) R. Costi, A. E. Saunders, U. Banin, *Angew. Chem.* **2010**, *122*, 4996 – 5016; *Angew. Chem. Int. Ed.* **2010**, *49*, 4878 – 4897; b) P. D. Cozzoli, T. Pellegrino, L. Manna, *Chem. Soc. Rev.* **2006**, *35*, 1195 – 1208; c) C. de Mello Donegá, *Chem. Soc. Rev.* **2011**, *40*, 1512 – 1546; d) C. Sanchez, B. Julian, P. Belleville, M. Popall, *J. Mater. Chem.* **2005**, *15*, 3559 – 3592.

[61] a) H. Wang, L. Chen, Y. Feng, H. Chen, *Acc. Chem. Res.* **2013**, *46*, 1636 – 1646; b) S. Torza, S. G. Mason, *J. Colloid Interface Sci.* **1970**, *33*, 67 – 83.

[62] S. Xing, L. H. Tan, M. Yang, M. Pan, Y. Lv, Q. Tang, Y. Yang, H. Chen, *J. Mater. Chem.* **2009**, *19*, 3286 – 3291.

[63] a) E. Bauer, *Z. Kristallogr.* **1958**, *110*, 372; b) S. E. Habas, H. Lee, V. Radmilovic, G. A. Somorjai, P. Yang, *Nat. Mater.* **2007**, *6*, 692 – 697.

[64] F.-R. Fan, D.-Y. Liu, Y.-F. Wu, S. Duan, Z.-X. Xie, Z.-Y. Jiang, Z.-Q. Tian, *J. Am. Chem. Soc.* **2008**, *130*, 6949 – 6951.

[65] a) L. J. Lauhon, M. S. Gudiksen, D. Wang, C. M. Lieber, *Nature* **2002**, *420*, 57 – 61; b) B. O. Dabbousi, J. Rodriguez-Viejo, F. V. Mikulec, J. R. Heine, H. Mattoussi, R. Ober, K. F. Jensen, M. G. Bawendi, *J. Phys. Chem. B* **1997**, *101*, 9463 – 9475; c) X. Peng, M. C. Schlamp, A. V. Kadavanich, A. P. Alivisatos, *J. Am. Chem. Soc.* **1997**, *119*, 7019 – 7029; d) J. J. Li, Y. A. Wang, W. Guo, J. C. Keay, T. D. Mishima, M. B. Johnson, X. Peng, *J. Am. Chem. Soc.* **2003**, *125*, 12567 – 12575.

[66] a) F. Caruso, *Adv. Mater.* **2001**, *13*, 11 – 22; b) Y. J. Wong, L. Zhu, W. S. Teo, Y. W. Tan, Y. Yang, C. Wang, H. Chen, *J. Am. Chem. Soc.* **2011**, *133*, 11422 – 11425; c) C. Xue, X. Chen, S. J. Hurst, C. A. Mirkin, *Adv. Mater.* **2007**, *19*, 4071 – 4074.

[67] a) Y. Kang, T. A. Taton, *Macromolecules* **2005**, *38*, 6115 – 6121; b) Y. Kang, T. A. Taton, *Angew. Chem.* **2005**, *117*, 413 – 416; *Angew. Chem. Int. Ed.* **2005**, *44*, 409 – 412; c) H. Y. Chen, S. Abraham, J. Mendenhall, S. C. Delamarre, K. Smith, I. Kim, C. A. Batt, *ChemPhysChem* **2008**, *9*, 388 – 392.

[68] S. Laurent, D. Forge, M. Port, A. Roch, C. Robic, L. Vander Elst, R. N. Muller, *Chem. Rev.* **2008**, *108*, 2064 – 2110.

[69] T. Pellegrino, L. Manna, S. Kudera, T. Liedl, D. Koktysh, A. L. Rogach, S. Keller, J. Radler, G. Natile, W. J. Parak, *Nano Lett.* **2004**, *4*, 703 – 707.

[70] a) A. Walther, A. H. E. Müller, *Chem. Rev.* **2013**, *113*, 5194 – 5261; b) J. Du, R. K. O'Reilly, *Chem. Soc. Rev.* **2011**, *40*, 2402 – 2416.

[71] Y. Feng, J. He, H. Wang, Y. Y. Tay, H. Sun, L. Zhu, H. Chen, *J. Am. Chem. Soc.* **2012**, *134*, 2004 – 2007.
[72] L. Zhang, A. Eisenberg, *J. Am. Chem. Soc.* **1996**, *118*, 3168 – 3181.
[73] B.-S. Kim, J.-M. Qiu, J.-P. Wang, T. A. Taton, *Nano Lett.* **2005**, *5*, 1987 – 1991.
[74] a) Y. Jin, X. Gao, *J. Am. Chem. Soc.* **2009**, *131*, 17774 – 17776; b) S. H. Hu, X. Gao, *J. Am. Chem. Soc.* **2010**, *132*, 7234 – 7237; c) Y. Jin, X. Gao, *Nat. Nanotechnol.* **2009**, *4*, 571 – 576.
[75] a) R. Bardhan, N. K. Grady, T. Ali, N. J. Halas, *ACS Nano* **2010**, *4*, 6169 – 6179; b) T. Pham, J. B. Jackson, N. J. Halas, T. R. Lee, *Langmuir* **2002**, *18*, 4915 – 4920; c) R. Bardhan, S. Mukherjee, N. A. Mirin, S. D. Levit, P. Nordlander, N. J. Halas, *J. Phys. Chem. C* **2009**, *114*, 7378 – 7383; d) Q. Zhang, J. Ge, J. Goebl, Y. Hu, Y. Sun, Y. Yin, *Adv. Mater.* **2010**, *22*, 1905 – 1909; e) H. Wang, D. W. Brandl, P. Nordlander, N. J. Halas, *Acc. Chem. Res.* **2006**, *40*, 53 – 62; f) C. Loo, A. Lin, L. Hirsch, M. H. Lee, J. Barton, N. J. Halas, J. West, R. Drezek, *Technol. Cancer Res. Treat.* **2004**, *3*, 33 – 40.
[76] H. Zhang, Y. J. Li, I. A. Ivanov, Y. Q. Qu, Y. Huang, X. F. Duan, *Angew. Chem.* **2010**, *122*, 2927 – 2930; *Angew. Chem. Int. Ed.* **2010**, *49*, 2865 – 2868.
[77] a) B. Lim, H. Kobayashi, T. Yu, J. G. Wang, M. J. Kim, Z. Y. Li, M. Rycenga, Y. N. Xia, *J. Am. Chem. Soc.* **2010**, *132*, 2506; b) J. Zeng, C. Zhu, J. Tao, M. S. Jin, H. Zhang, Z. Y. Li, Y. M. Zhu, Y. N. Xia, *Angew. Chem.* **2012**, *124*, 2404 – 2408; *Angew. Chem. Int. Ed.* **2012**, *51*, 2354 – 2358; c) C. Zhu, J. Zeng, J. Tao, M. C. Johnson, I. Schmidt-Krey, L. Blubaugh, Y. M. Zhu, Z. Z. Gu, Y. N. Xia, *J. Am. Chem. Soc.* **2012**, *134*, 15822 – 15831; d) X. H. Xia, Y. N. Xia, *Nano Lett.* **2012**, *12*, 6038 – 6042.
[78] a) M. R. Jones, K. D. Osberg, R. J. Macfarlane, M. R. Langille, C. A. Mirkin, *Chem. Rev.* **2011**, *111*, 3736 – 3827; b) C. R. Martin, *Chem. Mater.* **1996**, *8*, 1739 – 1746.
[79] a) J. Sarkar, G. G. Khan, A. Basumallick, *Bull. Mater. Sci.* **2007**, *30*, 271 – 290; b) G. Z. Cao, D. W. Liu, *Adv. Colloid Interface Sci.* **2008**, *136*, 45 – 64.
[80] B. Nikoobakht, M. A. El-Sayed, *Langmuir* **2001**, *17*, 6368 – 6374.
[81] C. Wang, Y. Hu, C. M. Lieber, S. Sun, *J. Am. Chem. Soc.* **2008**, *130*, 8902 – 8903.
[82] Y.-S. Chen, W. Frey, S. Kim, P. Kruizinga, K. Homan, S. Emelianov, *Nano Lett.* **2011**, *11*, 348 – 354.
[83] M. Yang, T. Chen, W. S. Lau, Y. Wang, Q. Tang, Y. Yang, H. Chen, *Small* **2009**, *5*, 198 – 202.
[84] Q. S. Wei, J. Ji, J. C. Shen, *Macromol. Rapid Commun.* **2008**, *29*, 645 – 650.
[85] Q. Li, R. Jiang, T. Ming, C. Fang, J. Wang, *Nanoscale* **2012**, *4*, 7070 – 7077.
[86] T. Chen, M. Yang, X. Wang, L. H. Tan, H. Chen, *J. Am. Chem. Soc.* **2008**, *130*, 11858 – 11859.
[87] a) J. Xu, Y. Wang, X. Qi, C. Liu, J. He, H. Zhang, H. Chen, *Angew. Chem.* **2013**, *125*, 6135 – 6139; *Angew. Chem. Int. Ed.* **2013**, *52*, 6019 – 6023; b) T. W. Hansen, A. T. Delariva, S. R. Challa, A. K. Datye, *Acc. Chem. Res.* **2013**, *46*, 1720 – 1730.
[88] a) L. Meli, P. F. Green, *Acs Nano* **2008**, *2*, 1305 – 1312; b) M. T. Swihart, *Curr. Opin. Colloid Interface Sci.* **2003**, *8*, 127 – 133; c) M. A. Asoro, D. Kovar, Y. Shao-Horn, L. F. Allard, P. J. Ferreira, *Nanotechnology* **2010**, *21*, 025701.
[89] a) M. Xiao, G. Xia, R. Wang, D. Xie, *Soft Matter* **2012**, *8*, 7865 – 7874; b) M. Li, H. Schnablegger, S. Mann, *Nature* **1999**, *402*, 393 – 395; c) H. Wang, Y.-T. Liu, H.-J. Qian, Z.-Y. Lu, *Polymer* **2011**, *52*, 2094 – 2101; d) M. Grzelczak, J. Vermant, E. M. Furst, L. M. Liz-Marzan, *ACS Nano* **2010**, *4*, 3591 – 3605.
[90] Z. Lu, Y. Yin, *Chem. Soc. Rev.* **2012**, *41*, 6874 – 6887.
[91] H. Wang, L. Chen, X. Shen, L. Zhu, J. He, H. Chen, *Angew. Chem.* **2012**, *124*, 8145 – 8149; *Angew. Chem. Int. Ed.* **2012**, *51*, 8021 – 8025.
[92] a) K. Liu, Z. Nie, N. Zhao, W. Li, M. Rubinstein, E. Kumacheva, *Science* **2010**, *329*, 197 – 200; b) X. Wang, G. Li, T. Chen, M. Yang, Z. Zhang, T. Wu, H. Chen, *Nano Lett.* **2008**, *8*, 2643 – 2647.
[93] a) M. Yang, G. Chen, Y. Zhao, G. Silber, Y. Wang, S. Xing, Y. Han, H. Chen, *Phys. Chem. Chem. Phys.* **2010**, *12*, 11850 – 11860; b) B. Derjaguin, *Kolloid-Z.* **1934**, *69*, 155 – 164.
[94] Z. Nie, D. Fava, E. Kumacheva, S. Zou, G. C. Walker, M. Rubinstein, *Nat. Mater.* **2007**, *6*, 609 – 614.
[95] Y. Wang, G. Chen, M. Yang, G. Silber, S. Xing, L. H. Tan, F. Wang, Y. Feng, X. Liu, S. Li, H. Chen, *Nat. Commun.* **2010**, *1*, 87.
[96] a) L. Zhang, A. Eisenberg, *Science* **1995**, *268*, 1728 – 1731; b) L. Zhang, K. Yu, A. Eisenberg, *Science* **1996**, *272*, 1777 – 1779; c) L. Zhang, A. Eisenberg, *Macromolecules* **1996**, *29*, 8805 – 8815.
[97] a) C. Lin, Y. Liu, S. Rinker, H. Yan, *ChemPhysChem* **2006**, *7*, 1641 – 1647; b) Y. Ofir, B. Samanta, V. M. Rotello, *Chem. Soc. Rev.* **2008**, *37*, 1814 – 1825; c) S. J. Tan, M. J. Campolongo, D. Luo, W. Cheng, *Nat. Nanotechnol.* **2011**, *6*, 268 – 276; d) S. Sotiropoulou, Y. Sierra-Sastre, S. S. Mark, C. A. Batt, *Chem. Mater.* **2008**, *20*, 821 – 834.
[98] Y. Huang, C.-Y. Chiang, S. K. Lee, Y. Gao, E. L. Hu, J. D. Yoreo, A. M. Belcher, *Nano Lett.* **2005**, *5*, 1429 – 1434.
[99] a) S. A. Davis, M. Breulmann, K. H. Rhodes, B. Zhang, S. Mann, *Chem. Mater.* **2001**, *13*, 3218 – 3226; b) Y. Ofir, B. Samanta, V. M. Rotello, *Chem. Soc. Rev.* **2008**, *37*, 1814 – 1823; c) S. I. Lim, C. J. Zhong, *Acc. Chem. Res.* **2009**, *42*, 798 – 808; d) Y. Y. Mai, A. Eisenberg, *Acc. Chem. Res.* **2012**, *45*, 1657 – 1666.
[100] a) C. B. Murray, C. R. Kagan, M. G. Bawendi, *Science* **1995**, *270*, 1335 – 1338; b) C. J. Kiely, J. Fink, M. Brust, D. Bethell, D. J. Schiffrin, *Nature* **1998**, *396*, 444 – 446; c) C. P. Collier, T. Vossmeyer, J. R. Heath, *Annu. Rev. Phys. Chem.* **1998**, *49*, 371 – 404; d) M. P. Pileni, *J. Phys. Chem. B* **2001**, *105*, 3358 – 3371; e) Z. L. Wang, *Adv. Mater.* **1998**, *10*, 13 – 30.
[101] a) A. S. Urban, X. Shen, Y. Wang, N. Large, H. Wang, M. W. Knight, P. Nordlander, H. Chen, N. J. Halas, *Nano Lett.* **2013**, *13*, 4399 – 4403; b) A. Sánchez-Iglesias, M. Grzelczak, T. Altantzis, B. Goris, J. Pérez-Juste, S. Bals, G. Van Tendeloo, S. H. Donaldson, B. F. Chmelka, J. N. Israelachvili, L. M. Liz-Marzán, *ACS Nano* **2012**, *6*, 11059 – 11065.
[102] a) D. J. Wales, H. A. Scheraga, *Science* **1999**, *285*, 1368 – 1372; b) R. S. Berry, *Chem. Rev.* **1993**, *93*, 2379 – 2394; c) D. J. Wales, J. P. K. Doye, M. A. Miller, P. N. Mortenson, T. R. Walsh, *Advances in Chemical Physics*, *Vol. 115* (Eds.: I. Prigogine, S. A. Rice), Wiley, New York, **2000**, pp. 1 – 111.
[103] a) Z. Zhuang, Q. Peng, B. Zhang, Y. Li, *J. Am. Chem. Soc.* **2008**, *130*, 10482 – 10483; b) P. Li, Q. Peng, Y. Li, *Chem. Eur. J.* **2011**, *17*, 941 – 946; c) Z. Huo, C. Chen, X. Liu, D. Chu, H. Li, Q. Peng, Y. Li, *Chem. Commun.* **2008**, 3741 – 3743; d) F. Bai, D. Wang, Z. Huo, W. Chen, L. Liu, X. Liang, C. Chen, X. Wang, Q. Peng, Y. Li, *Angew. Chem.* **2007**, *119*, 6770 – 6773; *Angew. Chem. Int. Ed.* **2007**, *46*, 6650 – 6653; e) Y. Nagaoka, O. Chen, Z. Wang, Y. C. Cao, *J. Am. Chem. Soc.* **2012**, *134*, 2868 – 2871; f) J. Zhuang, H. Wu, Y. Yang, Y. C. Cao, *J. Am. Chem. Soc.* **2007**, *129*, 14166 – 14167.
[104] a) Z. Quan, J. Fang, *Nano Today* **2010**, *5*, 390 – 411; b) T. Wang, J. Zhuang, J. Lynch, O. Chen, Z. Wang, X. Wang, D. LaMontagne, H. Wu, Z. Wang, Y. C. Cao, *Science* **2012**, *338*, 358 – 363; c) M. R. Jones, R. J. Macfarlane, B. Lee, J. A. Zhang, K. L. Young, A. J. Senesi, C. A. Mirkin, *Nat. Mater.* **2010**, *9*, 913 – 917.
[105] a) A. M. Kalsin, M. Fialkowski, M. Paszewski, S. K. Smoukov, K. J. M. Bishop, B. A. Grzybowski, *Science* **2006**, *312*, 420 – 424; b) E. V. Shevchenko, D. V. Talapin, N. A. Kotov, S. O'Brien,

C. B. Murray, *Nature* **2006**, *439*, 55 – 59; c) A. E. Saunders, B. A. Korgel, *ChemPhysChem* **2005**, *6*, 61 – 65.

[106] a) E. Auyeung, J. I. Cutler, R. J. Macfarlane, M. R. Jones, J. Wu, G. Liu, K. Zhang, K. D. Osberg, C. A. Mirkin, *Nat. Nanotechnol.* **2012**, *7*, 24 – 28; b) C. A. Mirkin, R. L. Letsinger, R. C. Mucic, J. J. Storhoff, *Nature* **1996**, *382*, 607 – 609; c) E. Auyeung, T. Li, A. J. Senesi, A. L. Schmucker, B. C. Pals, M. O. de La Cruz, C. A. Mirkin, *Nature* **2014**, *505*, 73 – 77; d) D. Nykypanchuk, M. M. Maye, D. van der Lelie, O. Gang, *Nature* **2008**, *451*, 549 – 552; e) R. J. Macfarlane, B. Lee, M. R. Jones, N. Harris, G. C. Schatz, C. A. Mirkin, *Science* **2011**, *334*, 204 – 208.

[107] a) L. Cademartiri, J. Bertolotti, R. Sapienza, D. S. Wiersma, G. von Freymann, G. A. Ozin, *J. Phys. Chem. B* **2005**, *110*, 671 – 673; b) Z. A. Peng, X. Peng, *J. Am. Chem. Soc.* **2002**, *124*, 3343 – 3353; c) B. Abécassis, F. Testard, O. Spalla, *Phys. Rev. Lett.* **2008**, *100*, 115504.

[108] Y. S. Xia, T. D. Nguyen, M. Yang, B. Lee, A. Santos, P. Podsiadlo, Z. Y. Tang, S. C. Glotzer, N. A. Kotov, *Nat. Nanotechnol.* **2011**, *6*, 580 – 587.

[109] a) Z. Tang, N. A. Kotov, *Adv. Mater.* **2005**, *17*, 951 – 962; b) T. Hu, Y. Gao, Z. L. Wang, Z. Y. Tang, *Front. Phys. China* **2009**, *4*, 487 – 496.

[110] a) K. K. Caswell, J. N. Wilson, U. H. F. Bunz, C. J. Murphy, *J. Am. Chem. Soc.* **2003**, *125*, 13914 – 13915; b) Z. Sun, W. Ni, Z. Yang, X. Kou, L. Li, J. Wang, *Small* **2008**, *4*, 1287 – 1292; c) S. Zhang, X. Kou, Z. Yang, Q. Shi, G. D. Stucky, L. Sun, J. Wang, C. Yan, *Chem. Commun.* **2007**, 1816 – 1818; d) T. Chen, H. Wang, G. Chen, Y. Wang, Y. Feng, W. S. Teo, T. Wu, H. Chen, *ACS Nano* **2010**, *4*, 3087 – 3094; e) N. Zhao, K. Liu, J. Greener, Z. Nie, E. Kumacheva, *Nano Lett.* **2009**, *9*, 3077 – 3081.

[111] a) K. Nakata, Y. Hu, O. Uzun, O. Bakr, F. Stellacci, *Adv. Mater.* **2008**, *20*, 4294 – 4299; b) G. A. DeVries, M. Brunnbauer, Y. Hu, A. M. Jackson, B. Long, B. T. Neltner, O. Uzun, B. H. Wunsch, F. Stellacci, *Science* **2007**, *315*, 358 – 361.

[112] B. Y. Kim, I.-B. Shim, O. L. A. Monti, J. Pyun, *Chem. Commun.* **2011**, *47*, 890 – 892.

[113] a) Z. Tang, N. A. Kotov, M. Giersig, *Science* **2002**, *297*, 237 – 240; b) M. Li, S. Johnson, H. Guo, E. Dujardin, S. Mann, *Adv. Funct. Mater.* **2011**, *21*, 851 – 859.

[114] M. Shim, P. Guyot-Sionnest, *J. Chem. Phys.* **1999**, *111*, 6955 – 6964.

[115] a) H. Xia, G. Su, D. Wang, *Angew. Chem.* **2013**, *125*, 3814 – 3818; *Angew. Chem. Int. Ed.* **2013**, *52*, 3726 – 3730; b) H. Zhang, D. Wang, *Angew. Chem.* **2008**, *120*, 4048 – 4051; *Angew. Chem. Int. Ed.* **2008**, *47*, 3984 – 3987.

[116] G. Gompper, M. Schick, *Soft Matter*, Wiley-VCH, Weinheim, **2007**, pp. 1 – 16.

[117] a) Y. Mai, A. Eisenberg, *Chem. Soc. Rev.* **2012**, *41*, 5969 – 5985; b) C. Cai, Y. Li, J. Lin, L. Wang, S. Lin, X.-S. Wang, T. Jiang, *Angew. Chem.* **2013**, *125*, 7886 – 7890; *Angew. Chem. Int. Ed.* **2013**, *52*, 7732 – 7736.

[118] L. Zhang, H. Shen, A. Eisenberg, *Macromolecules* **1997**, *30*, 1001 – 1011.

[119] a) C. Stoffelen, J. Voskuhl, P. Jonkheijm, J. Huskens, *Angew. Chem.* **2014**, *126*, 3468 – 3472; *Angew. Chem. Int. Ed.* **2014**, *53*, 3400 – 3404; b) H. Wang, S. Wang, H. Su, K.-J. Chen, A. L. Armijo, W.-Y. Lin, Y. Wang, J. Sun, K.-i. Kamei, J. Czernin, C. G. Radu, H.-R. Tseng, *Angew. Chem.* **2009**, *121*, 4408 – 4412; *Angew. Chem. Int. Ed.* **2009**, *48*, 4344 – 4348; c) C. Stoffelen, J. Huskens, *Chem. Commun.* **2013**, *49*, 6740 – 6742.

[120] D. E. Discher, A. Eisenberg, *Science* **2002**, *297*, 967 – 973.

[121] a) L. Chen, H. Shen, A. Eisenberg, *J. Phys. Chem. B* **1999**, *103*, 9488 – 9497; b) S. E. Burke, A. Eisenberg, *Langmuir* **2001**, *17*, 6705 – 6714.

[122] L. Zhang, C. Bartels, Y. Yu, H. Shen, A. Eisenberg, *Phys. Rev. Lett.* **1997**, *79*, 5034 – 5037.

[123] a) A. Blanazs, S. P. Armes, A. J. Ryan, *Macromol. Rapid Commun.* **2009**, *30*, 267 – 277; b) M. Antonietti, S. Förster, *Adv. Mater.* **2003**, *15*, 1323 – 1333; c) R. Nagarajan, *Langmuir* **2001**, *18*, 31 – 38.

[124] H. Shen, L. Zhang, A. Eisenberg, *J. Am. Chem. Soc.* **1999**, *121*, 2728 – 2740.

[125] D. J. Pochan, Z. Chen, H. Cui, K. Hales, K. Qi, K. L. Wooley, *Science* **2004**, *306*, 94 – 97.

[126] T. Azzam, A. Eisenberg, *Angew. Chem.* **2006**, *118*, 7603 – 7607; *Angew. Chem. Int. Ed.* **2006**, *45*, 7443 – 7447.

[127] a) S. Garnier, A. Laschewsky, *Colloid. Polym. Sci.* **2006**, *284*, 1243 – 1254; b) S. Jain, F. S. Bates, *Science* **2003**, *300*, 460 – 464.

[128] a) P. Alexandridis, J. F. Holzwarth, T. A. Hatton, *Macromolecules* **1994**, *27*, 2414 – 2425; b) G. Wanka, H. Hoffmann, W. Ulbricht, *Macromolecules* **1994**, *27*, 4145 – 4159.

[129] Z. Tuzar, P. Kratochvil, *Adv. Colloid Interface Sci.* **1976**, *6*, 201 – 232.

[130] a) H. Jin, W. Huang, X. Zhu, Y. Zhou, D. Yan, *Chem. Soc. Rev.* **2012**, *41*, 5986 – 5997; b) Y. Zhou, W. Huang, J. Liu, X. Zhu, D. Yan, *Adv. Mater.* **2010**, *22*, 4567 – 4590; c) Y. Zhou, D. Yan, *Chem. Commun.* **2009**, 1172 – 1188.

[131] O. Terreau, L. Luo, A. Eisenberg, *Langmuir* **2003**, *19*, 5601 – 5607.

[132] a) A. Rank, S. Hauschild, S. Förster, R. Schubert, *Langmuir* **2009**, *25*, 1337 – 1344; b) H. Tan, Z. Wang, J. Li, Z. Pan, M. Ding, Q. Fu, *ACS Macro Lett.* **2013**, *2*, 146 – 151; c) Y. Han, J. Cui, W. Jiang, *J. Phys. Chem. B* **2012**, *116*, 9208 – 9214; d) J. Cui, W. Jiang, *Langmuir* **2010**, *26*, 13672 – 13676; e) P. He, X. Li, D. Kou, M. Deng, H. Liang, *J. Chem. Phys.* **2010**, *132*, 204905; f) J. Cui, W. Jiang, *Langmuir* **2011**, *27*, 10141 – 10147; g) A. Blanazs, J. Madsen, G. Battaglia, A. J. Ryan, S. P. Armes, *J. Am. Chem. Soc.* **2011**, *133*, 16581 – 16587.

[133] H. Cui, Z. Chen, S. Zhong, K. L. Wooley, D. J. Pochan, *Science* **2007**, *317*, 647 – 650.

[134] J. Zhu, S. Zhang, K. Zhang, X. Wang, J. W. Mays, K. L. Wooley, D. J. Pochan, *Nat. Commun.* **2013**, *4*.

[135] a) A. H. Groschel, A. Walther, T. I. Lobling, F. H. Schacher, H. Schmalz, A. H. E. Muller, *Nature* **2013**, *503*, 247 – 251; b) R. C. Hayward, D. J. Pochan, *Macromolecules* **2010**, *43*, 3577 – 3584; c) A. H. Gröschel, F. H. Schacher, H. Schmalz, O. V. Borisov, E. B. Zhulina, A. Walther, A. H. E. Müller, *Nat. Commun.* **2012**, *3*, 710; d) J. H. Zhu, S. Y. Zhang, F. W. Zhang, K. L. Wooley, D. J. Pochan, *Adv. Funct. Mater.* **2013**, *23*, 1767 – 1773.

[136] Y. Yu, L. Zhang, A. Eisenberg, *Macromolecules* **1998**, *31*, 1144 – 1154.

